This is to certify that the

thesis entitled

NON-IMAGING ILLUMINATION USING
FIBER OPTICS

presented by

Ronald Thomas Kneusel

has been accepted towards fulfillment
of the requirements for

M.S. degree in Physics

O. L. Foiles

Major professor

Date 12/October/1993

NON-IMAGING ILLUMINATION USING FIBER OPTICS

By

Ronald Thomas Kneusel

A THESIS

Submitted to
Michigan State University
in partial fulfillment of the requirements
for the Degree of

MASTER OF SCIENCE

Department of Physics and Astronomy

1993

ABSTRACT

NON-IMAGING ILLUMINATION USING FIBER OPTICS

By

Ronald Thomas Kneusel

The use of fiber optics for controlled illumination is a relatively unexplored field. In this thesis, optical fibers of various sizes and materials were used to construct arrays that would be of potential use in automotive headlight systems. A zircon arc lamp simulated a bright point source and allowed careful control of the way the fiber arrays were illuminated. The subsequent patterns were analyzed alone and in conjunction with a cylindrical lens. This study showed that it would be possible to create a suitable headlight pattern with arrays of relatively few fibers and a few lenses, thereby reducing the physical size and complexity of current headlights.

For my wife, Maria, and my children David and Peter.

ACKNOWLEDGMENTS

The author would like to thank Dr. Carl Foiles for his guidance, patience and cheerful enthusiasm for this project.

The author also wishes to acknowledge the good people of FORD/PTPE(Plastic & Trim Products division) who first expressed interest in conducting and supporting this work. He hopes to see the final product under the hood of his car in the not too distant future.

Contents

List of Tables

List of Figures

Chapter 1

Introduction

1.1 Background information and Objective

An optical fiber is a dielectric waveguide designed to transmit electromagnetic energy at optical wavelengths. Optical fibers consist of a central core surrounded by a cladding layer which has a smaller index of refraction to allow for total internal reflection. Optical fibers were initially developed in the 1960s and have steadily improved in transmission quality since as is illustrated in Figure 1.1[Cherin1].

This thesis will explore the use of optical fibers in non-imaging illumination systems, in particular as might be used in an automotive headlight system, though the results can easily be applied to other situations. Three primary tasks were the focus of this research: testing the usefulness of a sum of Gaussian functions as an approximation to the light output from a linear array of fibers, measurement of the patterns produced by 1 and 2-dimensional arrays of line sources, and measurement of the line source as projected by a cylindrical lens. Each of these tasks applies directly to the use of fibers in non-imaging situations. A linear array of fibers is a logical building block for a headlight system, as is a cylindrical lens. For complete knowledge of the patterns produced by a linear array of fibers, a reasonable approximation to the functional form of a fiber's output must be available. A Gaussian is a logical first

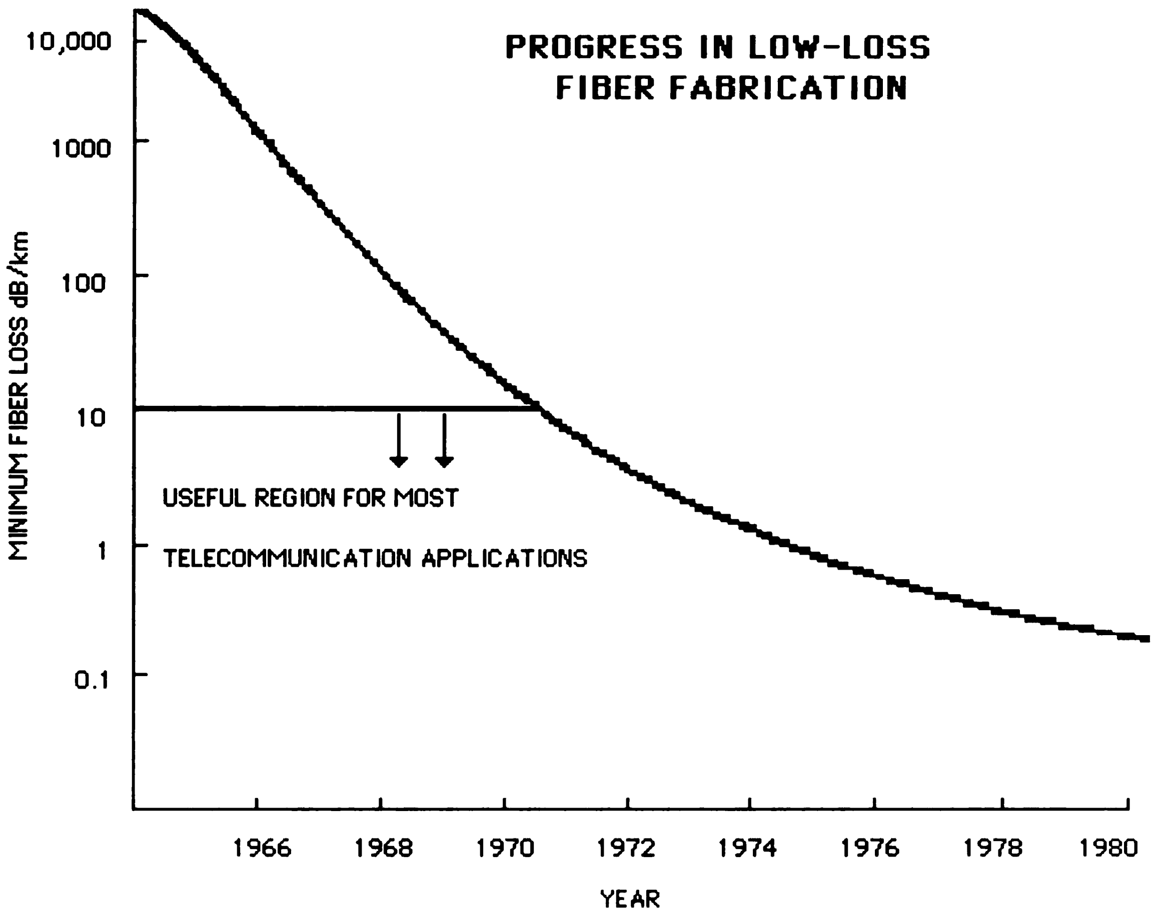

Figure 1.1: Progress in fiber fabrication [Cherin1].

approximation to this function.

1.2 Fiber Basics

1.2.1 Fiber modes

Since an optical fiber is a dielectric waveguide, the transmitted light energy must satisfy Maxwell's equations. The geometry involved produces a discrete set of propagating fields known as *modes.* Broadly speaking there are two classes of modes: *radiation* modes and *guided* modes [Newport2]. Radiation modes carry light energy out of the fiber core, hence, radiation modes are undesirable for most applications. Guided modes will propagate along the fiber axis transporting energy through the fiber. The number of guided modes is determined by the physical nature of the fiber but is primarily dependent upon the fiber's geometry. A larger core implies that a larger number of possible, simultaneous guided modes can exist. Which of the possible modes are excited depends on the way in which light is launched into the fiber. Factors that can determine launch conditions include the input light cone angle relative to the fiber axis, the size of the spot on the fiber face, and the axial concentration of light. For illumination purposes knowledge of exactly which modes are excited by which launch conditions is not an essential factor. It is sufficient to note that a very large number of modes can and will be excited in fibers with large ($d \sim 1$cm) diameters.

An arbitrary electromagnetic field launched into a fiber can be expressed as a linear superposition of the allowed fiber modes (a consequence of the orthogonal set of functions found as the solutions to Maxwell's equations). The energy initially distributed among the modes evolves in time, permitting a transfer between the various guided modes and even to radiation modes if the fiber is subjected to perturbations such as mircobending (caused by being pressed against a rough surface) or twisting. In the larger diameter fibers as would be used in a headlight system the above perturbations, unless severe, would not necessarily have a significant effect on the actual amount of light transmitted because of the great number of modes that would be excited. This contributes greatly towards lessening the difficulties that would be encountered during manufacture.

1.2.2 Types of fibers

Several types of optical fibers are available and are generally classified by their refractive index profile and physical diameter. Three broad categories exist: *multimode step-index*, *multimode graded-index*, and *single-mode* fibers [Newport3]. Figure 1.2 shows the three classes of fibers and their typical dimensions as commonly found in communications applications. The multimode fiber cores can be much larger than illustrated, and would be so in all but the smallest of illumination projects. These types will be discussed in turn to judge their usefulness in a fiber based illumination system.

Multimode step-index fibers are characterized by a large core with a constant refractive index. Fibers of this type with core diameters of up to 6.0mm were used in this project, and this would likely be the approximate size of a "first stage" to an automotive headlight. While undesirable for high rate, long distance communications applications because of their limited bandwidth (typically below 200 MHz·km), these fibers are inexpensive, have good light collecting abilities, and are easy to work with. This makes them an excellent choice for non-imaging illumination.

Multimode graded-index fibers consist of a smaller core, relative to the step-index fiber, whose refractive index gradually decreases in the radial direction. Their relatively large size and moderate bandwidth (between 200 MHz·km and 3 GHz·km)

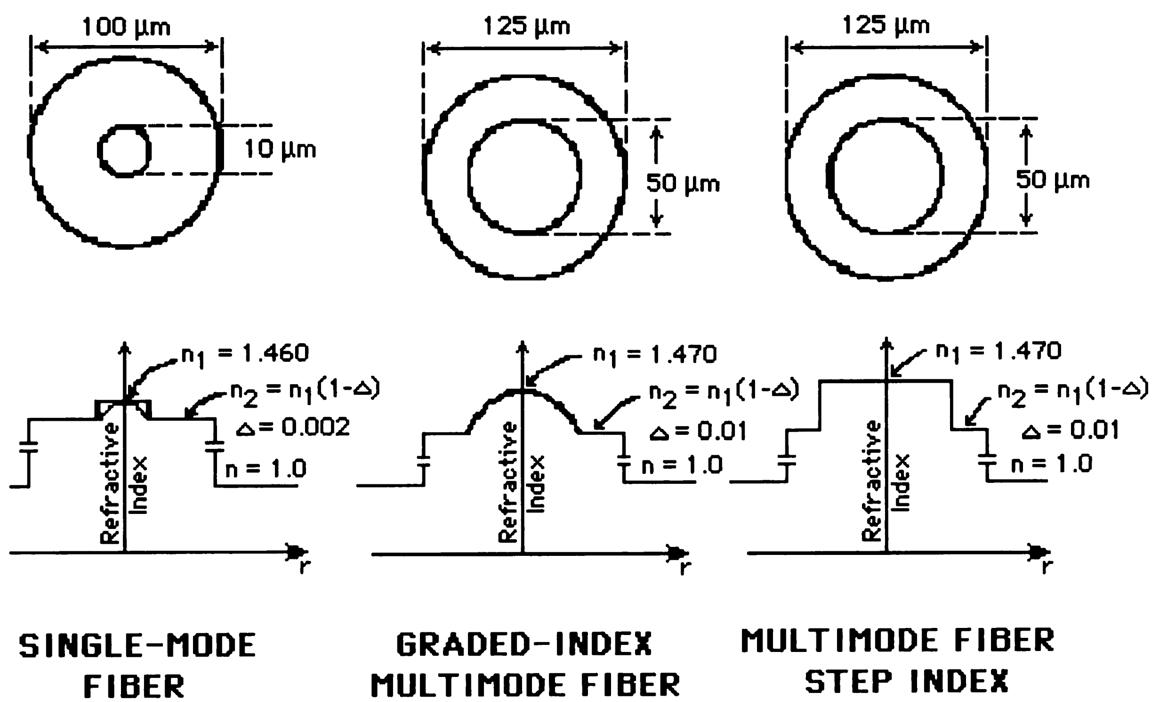

Figure 1.2: Geometry of fiber types [Cherin4].

make them a frequent choice for communications work, but their high manufacturing cost forbids their consideration in a headlight system.

The final fiber classification is the *single-mode* fiber. As its name implies, this fiber has only one propagating mode. In order to accomplish this the core needs to be on the order of 10 μm. While ideal for communications, indeed, they are the focus of virtually all research on fiber optics, their small cores and extreme difficulty in handling make them completely unsuited for illumination purposes.

Given the above choices of fibers for an illumination project, the logical choice is clear. The multimode step-index fiber is capable of being manufactured at a low cost (a major consideration for any commercial use) and can come in any size deemed necessary for a particular project.

1.2.3 Dispersion in fibers

Multimode fibers exhibit several types of dispersion that can affect bandwidth, the most significant of which is *modal dispersion* [Newport5]. The term modal dispersion is applied to two different effects. In the first, modal dispersion applies to the time differences which are, in a ray optics view, the result of differing path lengths for axial rays and oblique rays which undergo many reflections within the fiber. The second pertains to the distribution of light energy between the allowed modes of a fiber. In the first sense, modal dispersion is a function of fiber length and in systems with relatively short fibers is of little consequence. All other types of dispersions that affect fibers (notably material and waveguide dispersions) are orders of magnitude less than modal dispersion and can be safely ignored in large scale illumination systems, as an automotive headlight would be.

In the second sense, modal dispersion is not something that can be ignored and is a function of the launch conditions. This type of modal dispersion can affect the distribution of light coming out of a fiber and must be taken into account in a headlight system.

1.2.4 Attenuation in fibers

Attenuation of the energy propagating in a fiber is of extreme importance. Light energy decays exponentially with fiber length due to scattering and absorption. Scattering can couple energy from guided to radiation modes causing loss to occur. Scattering is caused by many factors. Rayleigh scattering arises from small fluctuations in the fiber's refractive index that are fixed in place during manufacture, producing the expected λ^{-4} dependence [Newport6]. Virtually any process that affects the fiber geometry will increase scattering and thereby increase attenuation. Absorption by impurities, most notably water, will also cause a loss of transmitted energy on a scale below that of scattering.

Scattering is of considerable importance in long range fiber communications, but is of little consequence in a lighting system that would use shorter lengths of larger diameter fibers where transmission efficiency is very high.

1.2.5 Useful parameters

When working with optical fibers it is often useful to make use of certain parameters. The numerical aperature (NA) is one such parameter. It is defined as the sine of the largest incident angle an incoming light ray may have and still be totally internally reflected in the fiber core, as is illustrated in Figure 1.3. Alternatively, the NA can be defined algebraically as:

$$NA = \sqrt{n_{core}^2 - n_{cladding}^2}$$

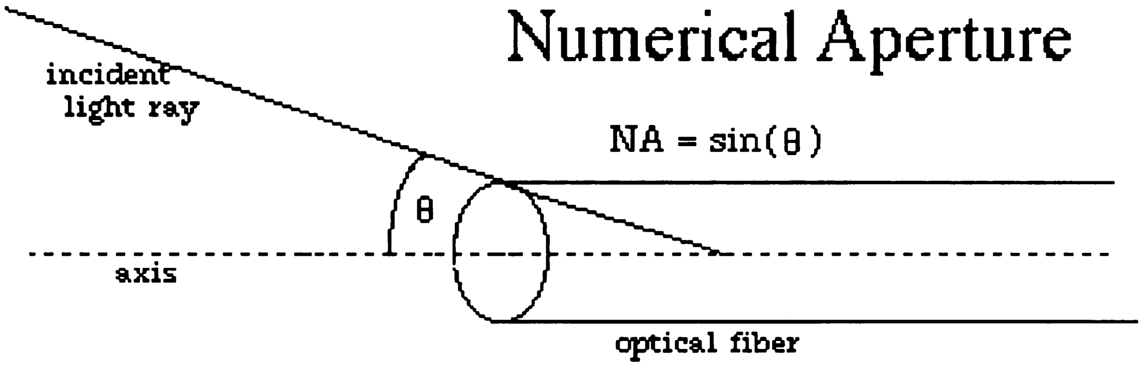

Figure 1.3: The geometrical definition of the Numerical Aperture (NA). The NA is the sine of the angle θ as shown. The angle θ ranged from 8.7^o to 33.0^o for the fibers used in this project.

where $n_{()}$ stands for the refractive index. Experimentally, the numerical aperture can be measured from the angle of the emitted light cone when all of the fiber's modes are excited. For the two sizes of fibers used in this project the NA was calculated to be 0.152 ($\theta = 8.7^o$) and 0.539 ($\theta = 33^o$) for the 1.0mm and 6.0mm diameter fibers respectively. It should also be noted that increasing the $n_{core}/n_{cladding}$ ratio will increase the NA for the same diameter, but at the expense of more scattering loss due to increased levels of dopant.

Another useful fiber parameter is the *normalized frequency parameter* or *V number*. It can be used to specify fiber characteristics such as the number of modes at a given wavelength, mode cut-off conditions (the frequency below which a given mode will no longer propagate), and propagation constants. In particular, for a multimode step-index fiber the number of guided modes at a given wavelength is approximately given by:

$$\textit{Number of modes} = V^2/2 \text{ [Newport7]}$$

Any fiber with $V \leq 2.405$ is a single-mode fiber.

The V number is defined as:

$$V = 2\pi NA(a/\lambda) = 2\pi(a/\lambda)\sqrt{n_{core}^2 - n_{cladding}^2}$$

where a is the fiber radius, λ is the wavelength, NA is the numerical aperature, and $n_{()}$ is the refractive index of the core and cladding respectively. For the two types of fibers used in this thesis, typical V numbers are (let $\lambda = 6328\mathring{A}$) $V \simeq 32,000$ and $V \simeq 752$ for the 6.0mm and 1.0mm diameter fibers. This leads to approximately 5.1×10^8 and 2.8×10^5 propagating modes respectively at this wavelength.

Chapter 2

Theory Specific to Prediction of Fiber Radiation Patterns

A gaussian is a logical first approximation to the radiation pattern produced by a single fiber. The use of a gaussian function facilitates the prediction of the behavior of extended sources built of single fibers as well. For the linear fiber arrays used in this project a simple summing of gaussian functions was used.

For a single multimode fiber in the HE_{11} mode the pattern produced follows the form

$$I(x) = e^{-ax^2}$$

[Newport8]. where $I(x)$ is the normalized intensity as a function of the radial distance perpendicular to the fiber axis and a is a parameter determined by experiment.

The HE_{11} mode is the fundamental mode and should be the dominant factor in determining the functional form of the realized output radiation pattern from a single fiber, therefore, the sum of many modes will tend to follow a Gaussian distribution as well.

A simple "brute force" summation of individual gaussian functions is a logical first approximation to the radiation patterns produced by linear arrays of fibers. Several statements then can be made concerning this summation: (1) the resultant radiation pattern will be constant over a range in x that is on the order of the size of the linear array, (2) the radiation pattern will be independent of the distance from the source, i.e., the functional form will still be Gaussian but with a different a parameter and (3) the summation will be valid in the plane perpendicular to the fiber axis when stacks of linear arrays are used.

An examination of the theoretical data presented in Figure 2.1 illustrates the expected radiation pattern using a summation of gaussian functions for a linear array of five fibers. The fiber-to-fiber spacing is 2.0mm.

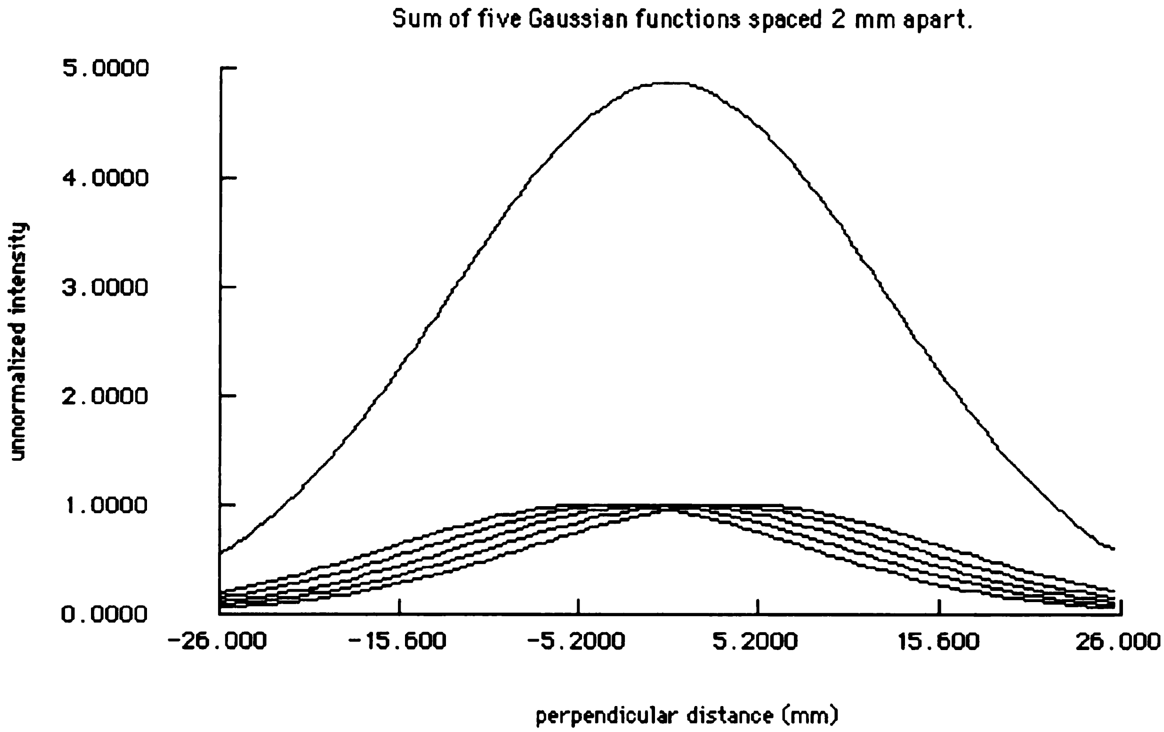

Figure 2.1: The expected theoretical radiation pattern for a linear array of five fibers. The top curve is the resultant pattern produced by summing the individual patterns (lower curves). This result has not been renormalized. Note the uniform intensity over a region on the order of the size of the fiber array.

Chapter 3

Experimental Procedure

3.1 Physical Set-up

Figure 3.1 illustrates in block form the basic experimental set-up. This arrangement can be divided into three major subsections: (1) the light source, (2) the coupling of light into the fiber arrays, and (3) the arrays themselves. This basic arrangement was sufficient to perform all the necessary measurements, and in a crude sense, directly models what would actually be found in a fiber based headlight system.

3.1.1 Light Source

Shielded 25 watt (or 100 watt) Zr arc lamps, whose output approximates a point source, were used in conjunction with a 50mm focal length converging lens to create a well defined, highly controllable light cone. This light cone was then launched into a 6.0mm diameter plastic fiber (1.7m in length). This fixed the launch conditions and isolated the light source from the fiber arrays. The distances from the lamp to the lens and from the lens to the fiber were adjusted to obtain the maximum power through the fiber. The transmission efficiency of the fiber was measured as a function of wavelength as outlined in Appendix A. The optimum lamp-lens-fiber distances were found to be: 75mm from lamp arc to lens and 95mm from lens to fiber surface.

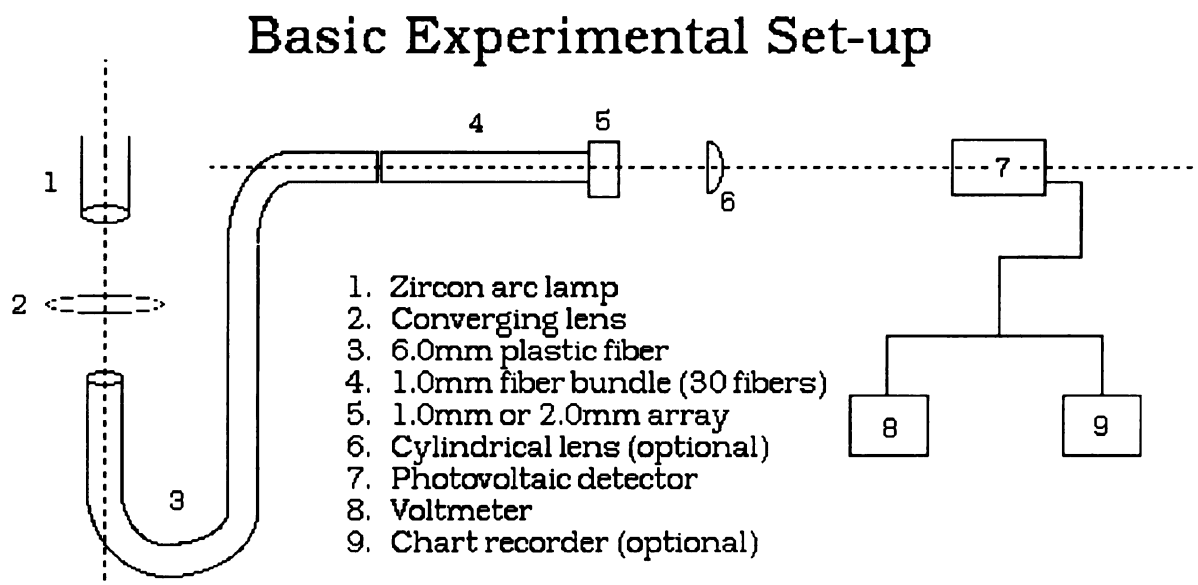

Figure 3.1: The basic experimental set-up. Note: parts 4 and 5 indicate the respective ends of the 1.0mm bundle, they are not two separate parts as suggested in the illustration.

These distances were fixed and remained constant throughout the experiment thereby assuring a fixed set of launch parameters for each subsequent measurement.

3.1.2 Coupling to Fiber Arrays

Coupling between the plastic fiber and the bundled input to the fiber arrays was accomplished by simple visual alignment. The bundled array input was of a slightly smaller diameter than the large plastic fiber (now used as a source) and was placed just away from its surface. Vertical alignment was fine tuned by raising or lowering the array input with an adjustable mount. Adjustments were made until all the array fibers were evenly illuminated, as determined by visual inspection. Then the array input was secured in place. This simple setup was quite good at providing the arrays with uniform illumination.

3.1.3 Fiber Arrays Used

Two different fiber arrays were used. Each was built of 1.0mm diameter plastic fibers arranged in a simple pattern. The individual fibers were made of a polystyrene core ($n = 1.159$) surrounded by a 10μm thick acrylic cladding ($n = 1.149$). The first array contained 30 such fibers (approximately 3 feet in length) in a 3 by 10 array with a center-to-center distance of 2.0mm as shown in Figure 3.2. The fibers were mounted in a block of clear plastic that had been drilled at 2.0mm intervals. The second array consisted of 31 fibers, each approximately 2.5 feet long, in three rows of 10, 11 and 10 fibers respectively as in Figure 3.3. The center-to-center distance was 1.0mm, the fibers were in direct contact with each other and the top and bottom rows were "stacked" in the spaces of the middle row. The fibers were then secured in this pattern. The opposite end of each array was made into a circular bundle which served as the input to the array. This input was then aligned with the output from

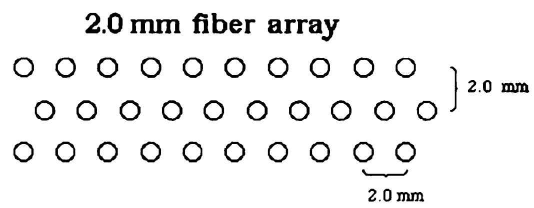

Figure 3.2: The 2.0mm fiber array.

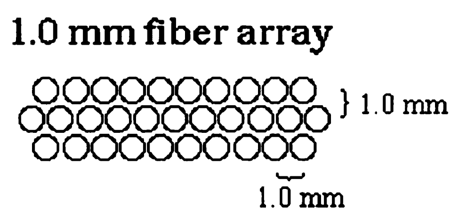

Figure 3.3: The 1.0mm fiber array.

the 6.0mm plastic fiber as described above.

3.2 Data Measurement

The light output from the fiber arrays was measured by a photovoltaic detector with several built-in apertures ranging in diameter from 3.0mm to 10.0mm and a built-in op amp providing four gain settings $(10^0, 10^1, 10^2, 10^3)$. The detector output, in volts, was calibrated with an industry standard laser power meter as described in Appendix B. A best fit of the calibration data gave a value of 0.9250 ± 0.0017 V/mW with virtually no offset.

The detector output was measured by either a voltmeter or a chart recorder. The voltmeter readings were used to create two-dimensional cross section plots of the output light distribution. Moving the detector at fixed distances both vertically and horizontally and entering the voltages thereby recorded into a computer produced low resolution 11 by 11 coded intensity plots similar to Figure 3.4. The detector was moved horizontally on a ruled platform set perpendicular to the optical axis and vertically by raising and lowering and by use of mounting rods of differing lengths. With appropriately sized steps and aperture the entire cross section (or a sample thereof if larger steps were used) could be measured. A distance of 125mm from the array fronts to the detector was maintained when no cylindrical lens was used. A distance of 80cm from the lens front to the detector was used if the lens was present. The output of each line array (row) was measured by masking the other two. This allowed for several measurements utilizing the same launch conditions and made reliable comparisons of the data possible. Pairs of rows were measured in a similar manner, and finally all three rows together were measured. Similar measurements were made for the individual line arrays after adding a cylindrical lens that was set

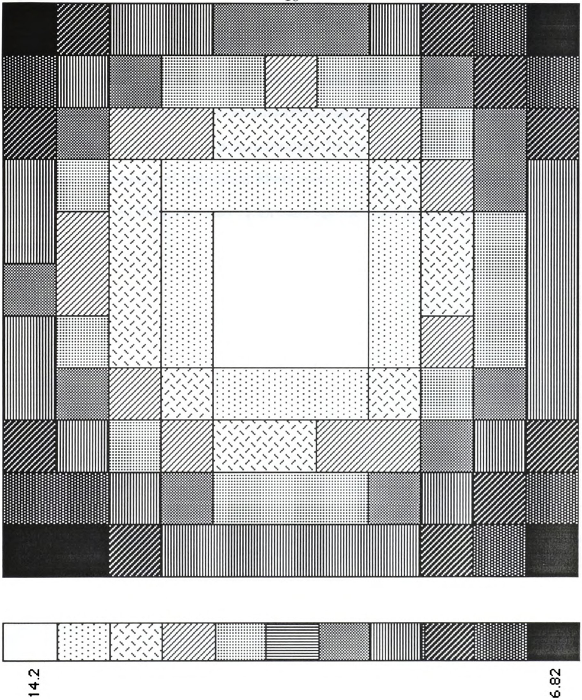

Figure 3.4: This sample 2-dimensional cross section from a fiber array is seen as if one were looking straight-on in front of the array. It is coded as indicated in the bar below the plot. Numerical values listed are the actual voltage in millivolts. The steps in this example are $\Delta x = \Delta y = 4.0$mm at a distance of 125mm from the 1.0mm fiber array.

at or near to its 44mm focal length.

A chart recorder and a motorized platform were used to produce continuous one-dimensional cross sections of the outputs from single fibers (or an entire row of fibers) similar to Figure 3.5 in order to help determine the functional form of the light output. Several measurements of individual fibers were taken by simply blocking the light from the unwanted fibers, thereby again assuring the same launch conditions for each measurement.

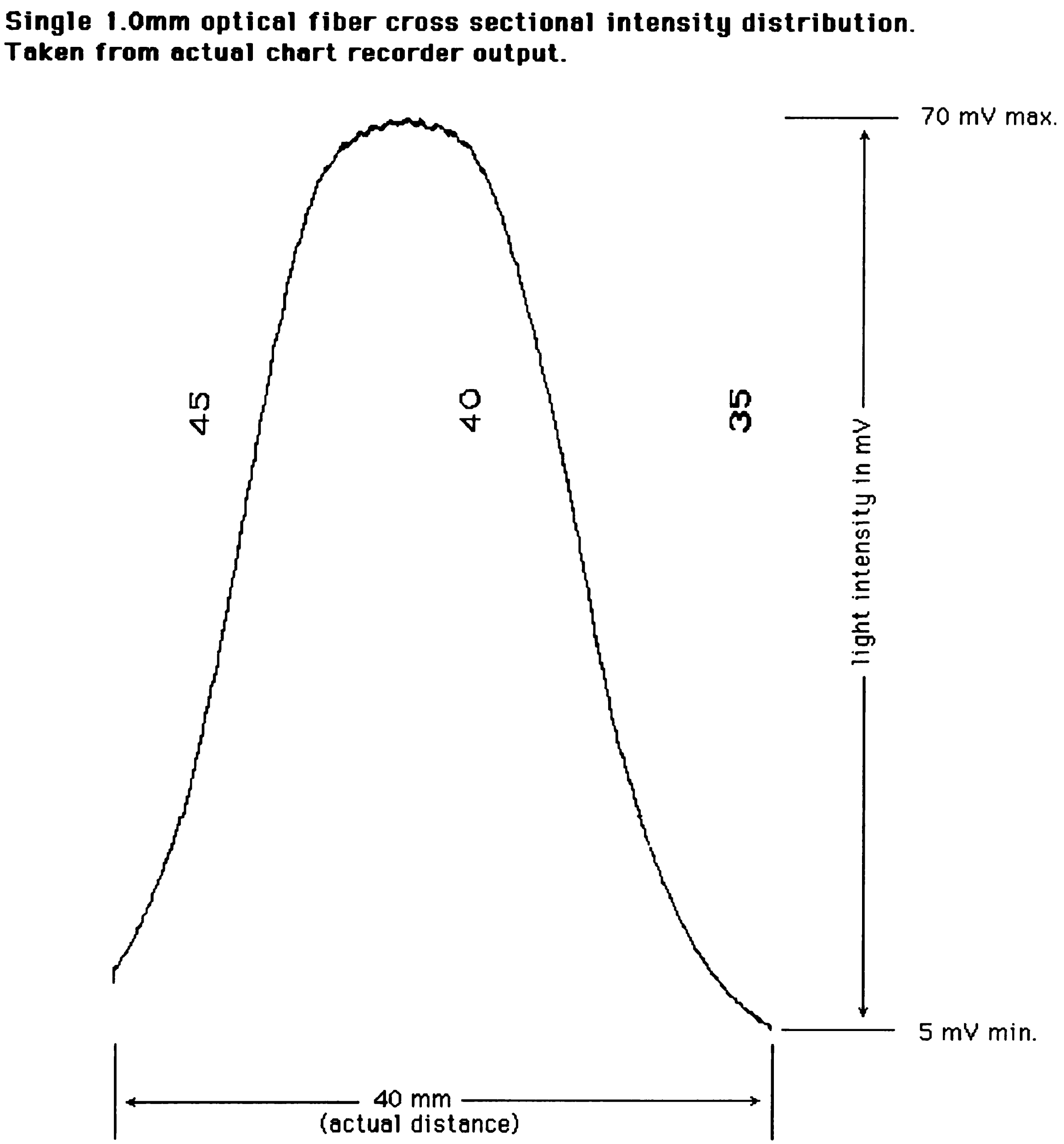

Figure 3.5: A sample 1-dimensional cross section from a single 1.0mm fiber. Taken with the chart recorder at a distance of 62mm.

Chapter 4

Experimental Results

Numerous tests and measurements were conducted to gain insight about the building of nonimaging systems. These tests consisted of measurements on (1) single fibers,(2) linear fiber arrays, (3) multiple linear fiber arrays, and (4) fiber arrays in conjunction with a cylindrical lens.

4.1 Explanation of Tabular Form

Many of the results to be presented are in tabular form and a description of said form is in order. The two dimensional cross section measurements were recorded by measuring the light intensity passing through a circular aperture at intervals which then were used to form an 11 by 11 grid. These individual measurements are referred to as cells. The step size was always greater than or equal to the diameter of the cell so that no overlap occured. For the majority of measurements which used step sizes of 4mm in both the vertical and horizontal directions the cells actually cover the light pattern completely.

Figures presented use either a table of numerical values, be they actual sampled voltages or percentage differences between tables, or a coded two dimensional cross section as in Figure 4.2. When viewing either the tables or the coded plots, it is important to bear the relationship between the $\hat{x}$ and $\hat{y}$ step sizes in mind. With the noted exception of the plots related to the cylindrical lens, the step size is the same in both directions and the plots appear with proper proportions. The coded two dimensional figures show what is seen when looking from the position of the fiber array itself out along the optical axis. The figures are also rotated such that when viewed on its side the $\hat{x}$ direction increases horizontally from left to right and the $\hat{y}$ direction increases vertically, from bottom to top.

4.2 Single Fiber Tests

In order to understand and model the effect of arrays of optical fibers it is necessary to develop a model for the simplest array: the single fiber. The light output from a single optical fiber (of the kind the arrays were constructed of) was measured with a chart recorder attached to a motorized photodiode detector moving perpendicular to the optical axis. The chart recorder provided a continuous one dimensional slice of the fiber's output which was used to determine its shape and to aid in finding a mathematical model for that shape.

After viewing the data obtained from the chart recorder it was decided that a Gaussian function was a logical point at which to start developing a model. To that end, the data from several different measurements of single fiber light output were fit to a standard three parameter Gaussian function. The results of the three parameter fit were further generalized to create a one parameter generic fit which was used to develop a model for linear arrays of fibers.

4.2.1 Three Parameter Gaussian Fit

The chart recorder data was taken at distances of 62mm and 125mm from the fiber face and the resulting curves were fitted to a Gaussian function of the form:

$$Y = A_0 \exp(-(X - A_1)^2/(2A_2^2))$$

The results of the fits are shown in Table 4.1. Comparison of the results given in Table 4.1 indicates that the ratio of $A_2(125)/A_2(62)$ is about 2.3 ± 0.1, some 15% greater than expected.

4.2.2 One Parameter Gaussian Fit

The results of the three parameter fit indicate that it is reasonable to assume $A_0 = 1.0$ and $A_1 = 0.0$ thereby reducing the three parameter Gaussian to a simpler form:

$$Y = \exp(-AX^2)$$

where $A = 1/(2A_2^2)$.

The generic parameter A derived from the results of Table 4.1 is given in Table 4.2 along with the final average A used as the basis for the generic fiber fit from which a model for linear arrays of fibers is based.

4.3 Single Linear Fiber Array Tests

Linear fiber arrays of ten or eleven fibers were constructed. The center to center fiber spacing was either 1.0mm or 2.0mm. The fiber arrays were oriented as indicated in Figure 4.1 and multiple cross sectional measurements of single arrays were taken. Cross sectional measurements of three 1.0mm arrays are shown in Figures 4.2,4.3 and 4.4.

Table 4.1: Results of Gaussian fit to single fiber cross section. The fit was confined to 10 degrees on either side of the optical axis.

Data Set	Distance (mm)	Parameters	$\pm 10°$
14	62.0	A_0	1.025 ± 0.048
		A_1	-0.264 ± 0.575
		A_2	9.3397 ± 0.575
13	62.0	A_0	1.019 ± 0.039
		A_1	0.291 ± 0.591
		A_2	10.969 ± 0.591
9	62.0	A_0	1.030 ± 0.046
		A_1	-0.568 ± 0.581
		A_2	9.8333 ± 0.581
5	125.0	A_0	1.013 ± 0.030
		A_1	-0.735 ± 1.06
		A_2	25.770 ± 1.06
11	125.0	A_0	0.996 ± 0.034
		A_1	-0.121 ± 1.09
		A_2	21.437 ± 1.09
12	125.0	A_0	1.000 ± 0.032
		A_1	-0.023 ± 1.04
		A_2	22.624 ± 1.04
Ave	62.0	A_0	1.0247 ± 0.0257
		A_1	-0.180 ± 0.336
		A_2	10.047 ± 0.336
	125.0	A_0	1.0030 ± 0.0185
		A_1	-0.293 ± 0.614
		A_2	23.277 ± 0.614

Table 4.2: Generic fit parameter A as derived from single fiber fits to a Gaussian function, $A = 1/2A_2^2$.

Data Set	Distance (mm)	A
9	62.0	$5.1710 \times 10^{-3} \pm 3.10 \times 10^{-4}$
13	62.0	$4.1556 \times 10^{-3} \pm 2.24 \times 10^{-4}$
14	62.0	$5.7320 \times 10^{-3} \pm 3.53 \times 10^{-4}$
5	125.0	$7.5293 \times 10^{-4} \pm 3.10 \times 10^{-5}$
11	125.0	$10.880 \times 10^{-4} \pm 5.53 \times 10^{-5}$
12	125.0	$9.7683 \times 10^{-4} \pm 4.50 \times 10^{-5}$
Average	62.0	$5.0195 \times 10^{-3} \pm 1.735 \times 10^{-4}$
	125.0	$9.3925 \times 10^{-4} \pm 2.591 \times 10^{-5}$

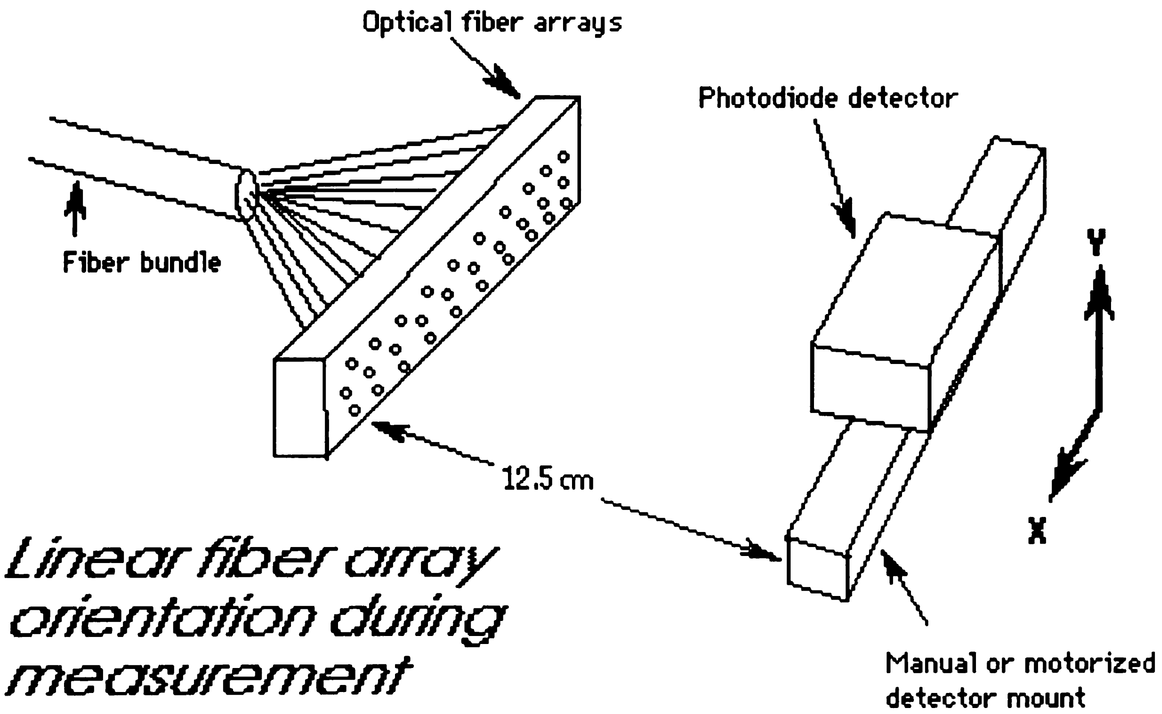

Figure 4.1: Linear fiber array orientation during measurement.

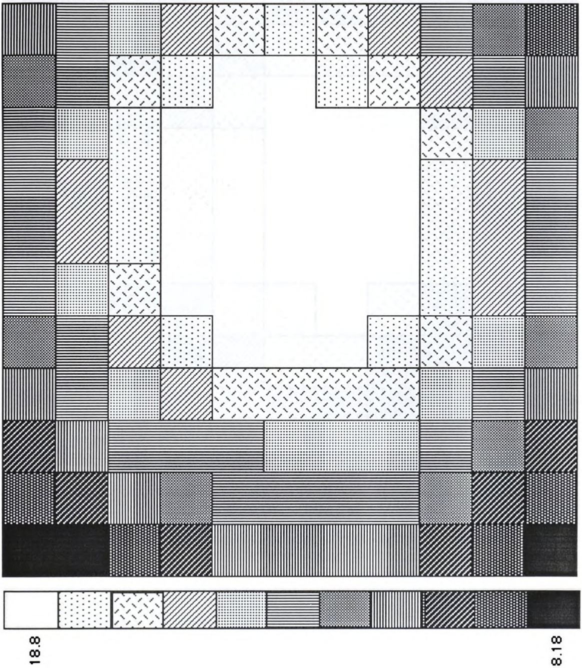

Figure 4.2: Linear array of 10 fibers in 2-d cross section. Taken at 125mm from the array face, each vertical ($\hat{x}$) and horizontal ($\hat{y}$) step represents a change of 4mm. Values listed are the light intensity in millivolts as given by the detector. This plot is from the top row of the 1.0mm fiber array.

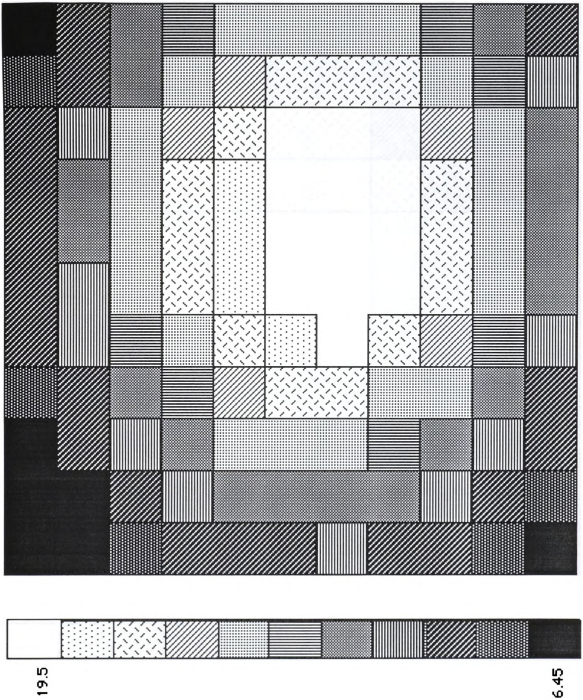

Figure 4.3: Linear array of 11 fibers in 2-d cross section. Taken at 125mm from the array face, each vertical ($\hat{x}$) and horizontal ($\hat{y}$) step represents a change of 4mm. Values listed are the light intensity in millivolts as given by the detector. This plot is from the middle row of the 1.0mm fiber array.

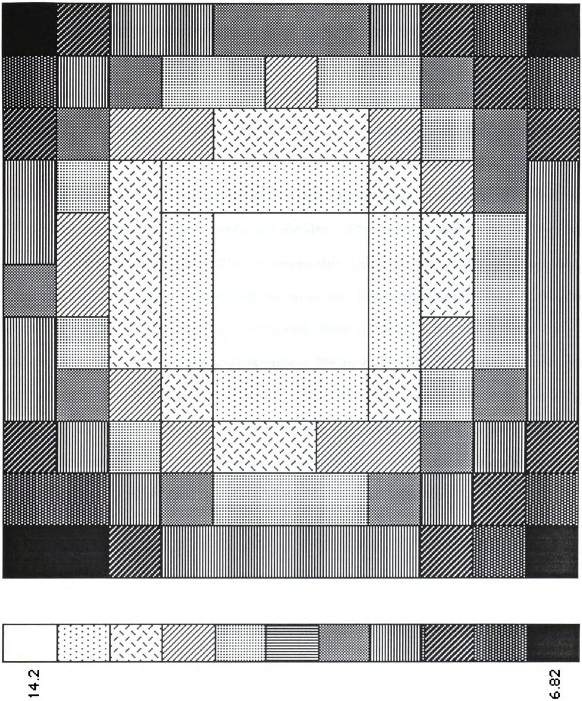

Figure 4.4: Linear array of 10 fibers in 2-d cross section. Taken at 125mm from the array face, each vertical ($\hat{x}$) and horizontal ($\hat{y}$) step represents a change of 4mm. Values listed are the light intensity in millivolts as given by the detector. This plot is from the bottom row of the 1.0mm fiber array.

When considered in numerical form, the above plots can be used to generate a table of percentage differences for the same array measurements as an indication of the reproducibility of the results. Table 4.3 shows the percentage difference between Figure 4.2 and Figure 4.3 for the 1.0mm array. The seemingly large differences at the edge of the pattern are due to the small values measured in that region. Similarly, Table 4.4 shows the percent difference for two 2.0mm array measurements. Percent differences for other measurements are similar. The percent difference is large at the edges of the tables but within a reasonable value at the center of the table. The width of each table corresponds to an actual perpendicular distance of 40mm while the length of each array was 10mm and 20mm for the 1.0mm and 2.0mm arrays respectively. Each table spans approximately 40mm vertically while the actual arrays are 1.0mm in height. For the array with a 1.0mm fiber spacing the difference is within $\pm 5\%$ over an area that is on the order of the physical array size, but increases rapidly outside this range. The 2.0mm arrays are inconsistent over the entire range measured. This effect will be discussed in greater detail in the next chapter.

Table 4.3: The percent difference in light intensity between two linear fiber arrays with a 1.0mm center-to-center spacing. The value listed is such that a negative number indicates the first measurement has a smaller value in that cell than the second. The decision as to which is first or second is arbitrary. The difference is taken from the actual detector output for that cell. The seemingly large differences at the edge of the pattern are due to the small values measured in that region. The – are the result of matching the data sets.

–	–	-14.3	-22.2	-30.0	-36.4	-41.7	-46.2	-50.0	-57.1	-61.5
–	–	0.0	-10.0	-18.2	-23.1	-28.6	-33.3	-43.8	-50.0	-53.3
–	–	11.1	0.0	-7.7	-13.3	-18.8	-23.5	-33.3	-44.4	-50.0
–	–	20.0	16.7	7.1	6.2	-5.6	-15.8	-21.1	-35.0	-42.1
–	–	27.3	30.8	35.7	17.6	5.3	-5.0	-15.0	-25.0	-35.0
–	–	45.5	38.5	26.7	17.6	5.3	0.0	-5.0	-15.0	-30.0
–	–	45.5	38.5	33.3	23.5	10.5	5.0	0.0	-10.0	-15.8
–	–	45.5	38.5	33.3	23.5	16.7	10.5	5.3	0.0	-10.5
–	–	60.0	58.3	42.9	40.0	23.5	16.7	5.6	0.0	-11.8
–	–	66.7	80.0	58.3	42.9	33.3	25.0	12.5	0.0	-6.7
–	–	85.7	66.7	70.0	63.6	50.0	38.5	23.1	7.7	0.0

4.4 Multiple Linear Fiber Array Tests

Fiber arrays were stacked horizontally and the net light pattern from pairs or sets of three were measured. Two fiber arrays were constructed, one with a 1.0mm center-to-center fiber spacing and the other with a 2.0mm spacing. The net light intensity was measured as a cross section in the same manner as the single fiber arrays. In the following, top row refers to the uppermost linear array, etc. The generic term array refers to the actual physical block of three linear arrays.

Figure 4.5 illustrates the net pattern from the top and middle rows of the 1.0mm fiber array. Note that the vertical spacing between the two rows was 1.0mm. The subsequent figures, Figure 4.6, Figure 4.7 and Figure 4.8 represent the combinations measured. These will be compared to the approximations arrived at by summing appropriately spaced Gaussian functions. Note that the vertical spacing between the top and bottom rows of the 1.0mm (2.0mm) array was 2.0mm (4.0mm). The measurements were taken with the photodiode detector sampling the same region of space regardless of which rows were actually being used.

4.5 Fiber Arrays in Conjunction with a Cylindrical Lens

Cylindrical lenses are useful for concentrating the light output from extended line sources. This concentrating effect was measured for single linear arrays of fibers. At all times the lens used was of sufficient length to completely cover the row of fibers and assure that all the light from the fibers passed through the lens.

Table 4.5 shows the light pattern generated by a single row of ten fibers with a 1.0mm spacing. The pattern was measured at a distance of 80cm from the array face with a horizontal cell spacing of 60.0mm and a vertical cell spacing of 3.0mm. The

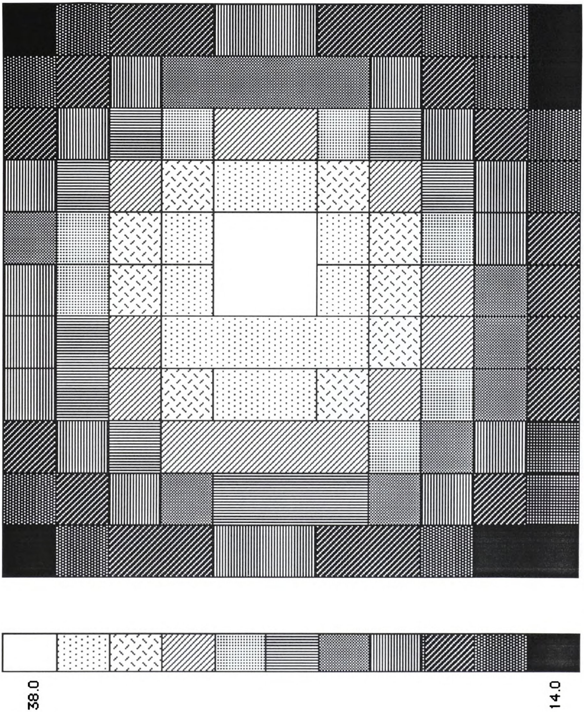

Figure 4.5: Cross sectional plot of the net light intensity from two linear arrays of fibers. The vertical and horizontal fiber spacing was 1.0mm. The cross section is seen as if facing the arrays.

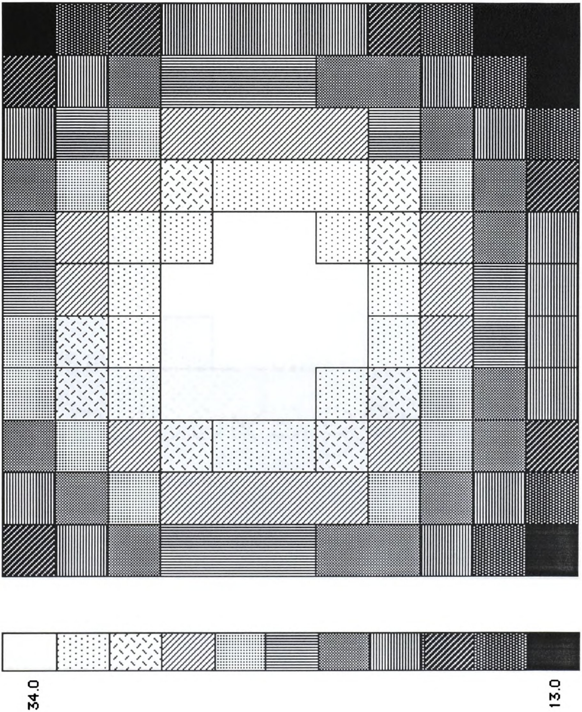

Figure 4.6: Cross sectional plot of the net light intensity from two linear arrays of fibers. The vertical spacing was 2.0mm and the horizontal spacing was 1.0mm. The cross section is seen as if facing the arrays.

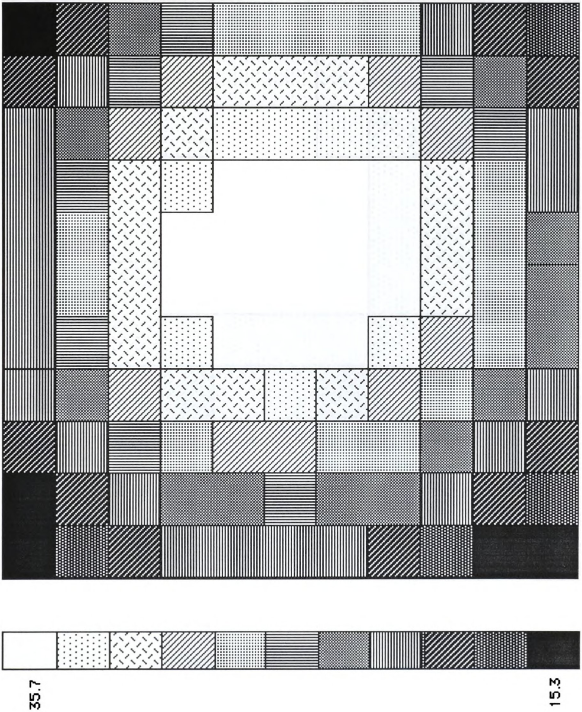

Figure 4.7: Cross sectional plot of the net light intensity from two linear arrays of fibers. The vertical and horizontal spacing was 2.0mm. The cross section is seen as if facing the arrays.

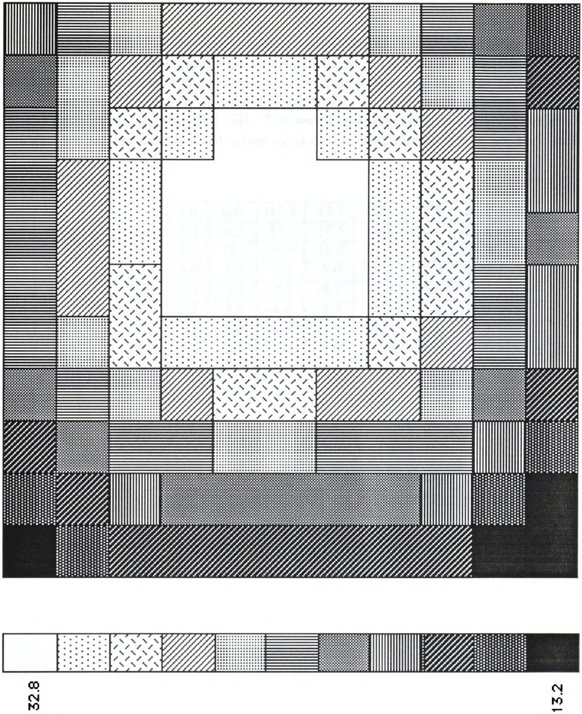

Figure 4.8: Cross sectional plot of the net light intensity from two linear arrays of fibers. The vertical spacing was 4.0mm and the horizontal spacing was 2.0mm. The cross section is seen as if facing the arrays.

Table 4.4: The percent difference in light intensity between two linear fiber arrays with a 2.0mm center-to-center spacing. The value listed is such that a negative number indicates the first measurement has a smaller value in that cell than the second. The decision as to which is first or second is arbitrary. The difference is taken from the actual detector output for that cell. The seemingly large differences at the edge of the pattern are due to the small values measured in that region. The – are the result of matching the data sets.

14.3	12.5	0.0	0.0	0.0	-15.4	-15.4	-23.1	-25.0	-20.0	-22.2
0.0	10.0	0.0	-7.1	-6.7	-17.6	-17.6	-18.8	-20.0	-15.4	-18.2
20.0	8.3	7.1	-5.9	-10.5	-15.0	-15.0	-21.1	-17.6	-20.0	-23.1
9.1	0.0	-6.2	-5.6	-5.3	-5.0	-5.0	-10.0	-15.8	-11.8	-14.3
9.1	7.7	0.0	0.0	-5.0	-9.5	-9.5	-14.3	-15.0	-16.7	-18.8
18.2	15.4	6.2	0.0	-5.0	-4.8	-4.8	-9.5	-15.0	-21.1	-23.5
9.1	0.0	6.2	-5.3	-5.0	-4.8	-4.8	-9.5	-10.5	-16.7	-13.3
9.1	7.7	6.7	-5.6	0.0	-5.0	-5.0	-15.0	-11.1	-12.5	-14.3
10.0	18.2	15.4	6.7	0.0	-5.6	-5.6	-11.1	-6.2	-7.1	-8.3
–	–	–	–	–	–	–	–	–	–	–
–	–	–	–	–	–	–	–	–	–	–

sum of each of the rows and columns is listed along with the net sum. The values listed are in millivolts as read from the detector output.

Table 4.6 shows the light pattern generated by the same array of fibers with the light first passing through a cylindrical lens placed at its focal length (f = 44mm) from the fibers.

Table 4.5: Cross section from a single row of fibers with a 1.0mm spacing. The pattern was measured at a distance of 800mm from the array face with horizontal and vertical cell spacings of 60mm and 3.0mm respectively. The sum of each row and column is listed as well as the net sum.

14	17	23	32	41	44	42	35	25	19	15	307
13	17	23	32	41	44	42	35	25	19	15	306
14	17	23	32	41	44	42	34	25	19	15	306
14	17	23	32	41	44	42	35	25	19	15	307
14	17	23	32	41	44	42	34	25	19	15	306
13	17	23	32	41	44	42	34	25	19	15	305
14	17	23	32	41	44	42	35	26	19	15	308
14	17	23	32	41	44	42	35	25	19	15	307
13	17	23	32	41	43	42	34	26	20	16	307
13	17	23	31	40	43	42	34	25	19	16	303
13	17	23	32	40	43	41	34	25	19	15	302
149	187	253	351	449	481	461	379	277	210	167	3364

Table 4.6: Cross section from a single row of fibers with a 1.0mm spacing. The pattern was measured at a distance of 800mm from the array face with horizontal and vertical cell spacings of 60mm and 3.0mm respectively. The sum of each row and column is listed as well as the net sum. The cylindrical lens was at $f = 44$mm.

30	30	40	50	50	50	60	50	40	40	30	470
30	40	50	60	70	70	70	70	60	40	30	590
30	40	60	80	90	100	100	90	70	50	30	740
40	60	90	120	160	170	170	140	100	60	40	1150
40	60	110	180	260	300	270	200	120	70	40	1650
40	70	140	250	360	410	360	260	140	80	40	2150
40	80	150	270	410	460	410	280	150	80	40	2370
40	80	150	270	410	460	410	290	150	80	40	2380
40	70	130	220	320	360	330	230	130	70	40	1940
40	60	100	140	190	210	200	160	100	60	40	1300
30	50	70	100	120	130	130	110	80	50	40	910
400	640	1090	1740	2440	2720	2510	1880	1140	680	410	15650

Chapter 5

Discussion

5.1 A Gaussian as a Model of the Light Output from a Single Fiber

To successfully model the light output of a nonimaging fiber optic system it is necessary to have an accurate model of the light output of a single optical fiber. Much of the present research and analysis was concerned with finding a simple yet useful model for the light output from a single optical fiber of the kind that might be used in a nonimaging system. The light from a single fiber was measured in cross section and then fitted to a Gaussian function as an approximation to the true distribution. The fit was reduced to a single parameter, the results of which were given in Table 4.2. This single parameter Gaussian was used as the "Gaussian model" and formed the basis for the simulated data used below. Figure 5.1 and Figure 5.2 show the average of the single parameter fits at 62mm and 125mm from the face of the fiber. The data sets with the greatest deviation from the average are plotted as an indication of the variation in the fits.

5.2 Building Linear Fiber Arrays with the Gaussian Model

Figure 5.3 illustrates the predicted and the average intensity of two separate measurements of the light from a linear array of 10 fibers with a 1.0mm spacing at a distance of 125.0mm from the face of the fiber array. The agreement is reasonable out to a distance of about 10mm from the optical axis, corresponding to an angle of approximately 4.5 degrees. After this point the light intensity falls off faster than the Gaussian model. Similarly, Figure 5.4 shows the average of three arrays of 10 fibers that are 2.0mm apart. Again, the model is useful to approximately 4.5 degrees from the optical axis. The usefulness of the Gaussian model for detailed analysis is limited by this rapid divergence from the true distribution. The data for these graphs was generated by Program 2 listed in Appendix C.

Another computer program, the source code of which is listed in Appendix C as Program 1, was used to generate a two dimensional grid of the predicted, normalized light distribution from a linear array of 10 fibers with either a 1mm or 2mm center-to-center spacing based on the Gaussian model. The program used the model for a single fiber to calculate the light intensity at a point where data was measured. It then summed the intensities for all the fibers in the array. This was done for each point at which data was measured. The predicted intensities were then normalized. This simulated data was compared with data from actual cross sections and the percent difference from the simulated data was calculated. Table 5.1 shows a typical result for a linear array of 10 fibers with a 1.0mm spacing. Table 5.2 is a typical result for an array with a 2.0mm center-to-center spacing. From these tables it is clear that the Gaussian model is not sufficient for detailed simulation of the light from linear arrays of fibers. It works well near the center of the image, but becomes increasingly

unacceptable as the distance from the center increases. However, the model is useful for reproducing the general form of the light output and therefore of value when rough modeling is sufficient.

5.3 Summing Linear Arrays of Fibers

5.3.1 Normalized Intensity of Actual and Simulated Arrays

Multiple linear arrays were built of three linear arrays placed one on top of the other, and are hereafter called a bundle. The vertical spacing equaled the horizontal spacing between the fibers in the linear array, either 1.0mm or 2.0mm. Table 5.3 gives the cell-by-cell percent difference between the 1.0mm bundle and the simulated light output for three linear based on the Gaussian model. The data was normalized. Table 5.4 gives the same information for the 2.0mm bundle. The percent difference was found using Program 4 in Appendix C.

As with the linear arrays, the Gaussian model works well near the center of the image, but becomes unreliable further way from the center.

5.3.2 Normalized Intensity of Actual and Sum of Actual Arrays

Table 5.5 gives the percent difference of the normalized intensity from a measurement of the light from the 1.0mm bundle and the sum of the normalized light from measurements of the individual linear arrays of which the 1.0mm bundle is constructed. Table 5.6 gives the same comparison for arrays with 2.0mm spacing.

It is clear that there is not a significant difference between the simulated and actual measurements when considered in this form. However, normalization involves the loss of information and only indicates the form of the light distribution, not the intensity. A differenct picture emerges when looking at direct sums of the absolute intensity.

5.3.3 True Intensity of Actual and Sum of Actual Arrays

One would expect the light measured from a bundle to be comparable to the sum of the light from the individual arrays from which the bundle is constructed. Table 5.7 shows the percent difference between the actual values measured from the 1mm bundle and the sum of the individual 1mm linear arrays that make up the bundle. Table 5.8 shows the same information for the 2.0mm bundle. The cause for the large difference between the actual data and the sum of the individual arrays is not clearly understood. Possible causes are discussed in the next section.

5.4 Possible Sources for Observed Differences Between Measurements

As noted in the previous chapter, there were large percent differences found between subsequent measurements of the two dimensional cross sections from single linear fiber arrays. Table 4.3 and Table 4.4 show the order of percent difference that was typical between measurements. Possible sources for these differences include (1) inconsistent illumination of the fiber array and (2) incomplete masking of the light from other fiber arrays.

Light from the source lamp was focused into a 6mm diameter plastic fiber, the output of which was sent into the bundled end of the fibers that formed the arrays. The large fiber and the bundled end were placed end to end. Alignment was accomplished visually, adjusting until the fibers appeared to be most evenly illuminated. Sensitivity of the illuminated array fibers to the launch conditions perhaps resulted in changes in the illumination that while not directly visible were within the range of the photodiode detector. Most measurements were made on different days, often following an adjustment of the equipment which would have changed the launch conditions.

A second source could have been the mask used to block the light from arrays that were not being measured. The linear arrays were set in a block of plastic, one on top of the other. To isolate a specific array it was necessary to mask the other two. The mask was constructed of black plastic and placed over the arrays that were to be blocked. If the mask was not fully covering the light from one of the other arrays that light would add to the measured data.

The above sources, either alone or together, could account for the differences observed.

5.5 Shaping the Light Pattern with a Cylindrical Lens

Tables 4.5 and 4.6 demonstrate the ability of a single cylindrical lens to affect the light output from a linear array of fibers. The simple addition of a cylindrical lens at its focal point caused an intensity increase by a factor of 4.65 over the entire region measured and an increase by a factor of 8.0 in the central region within 10mm vertically and 100mm horizontally. The greatest concentrating of the light was found when the array was placed at the focal point of the lens. The source code for the program that summed the intensities is listed in Appendix C as Program 3.

This ability to greatly concentrate the light in one dimension makes cylindrical lenses a useful tool for working with fiber systems. A comparison of the pattern produced with the array and cylindrical lens to the pattern required for a low-beam headlight in an automobile is given in the next chapter.

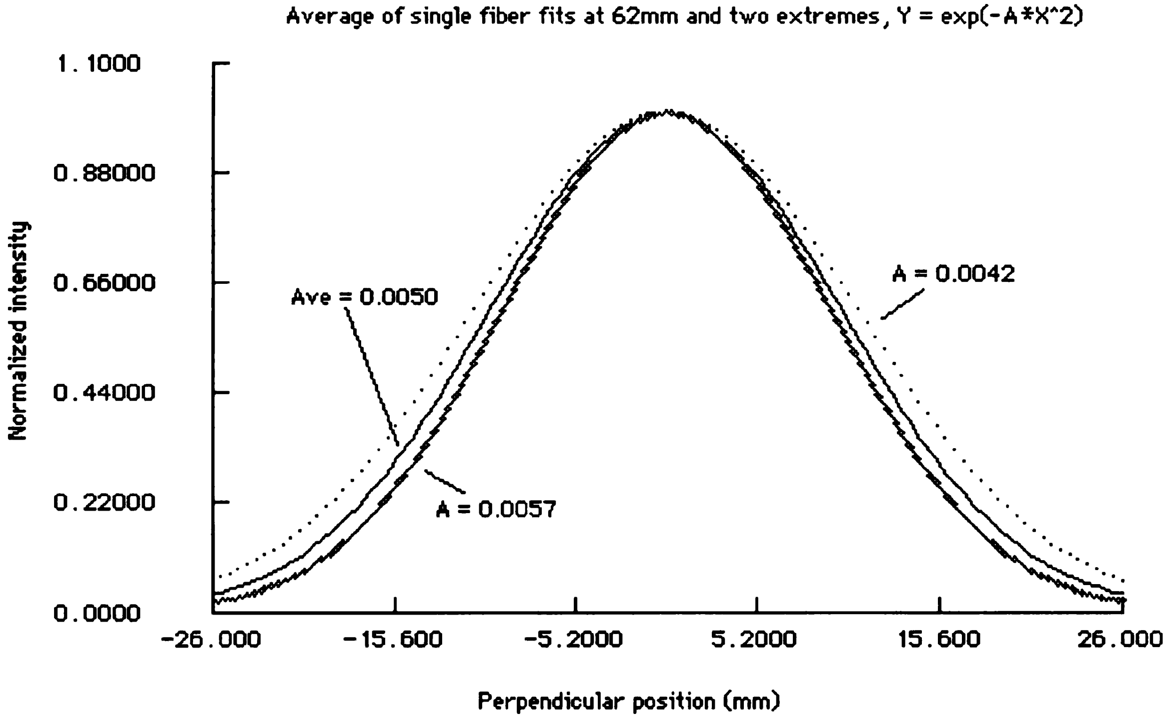

Figure 5.1: One parameter Gaussian fit to the light output from a single fiber. Plotted are the average and two extremes fits at 62mm from the fiber face. Values given are for the generic fit parameter.

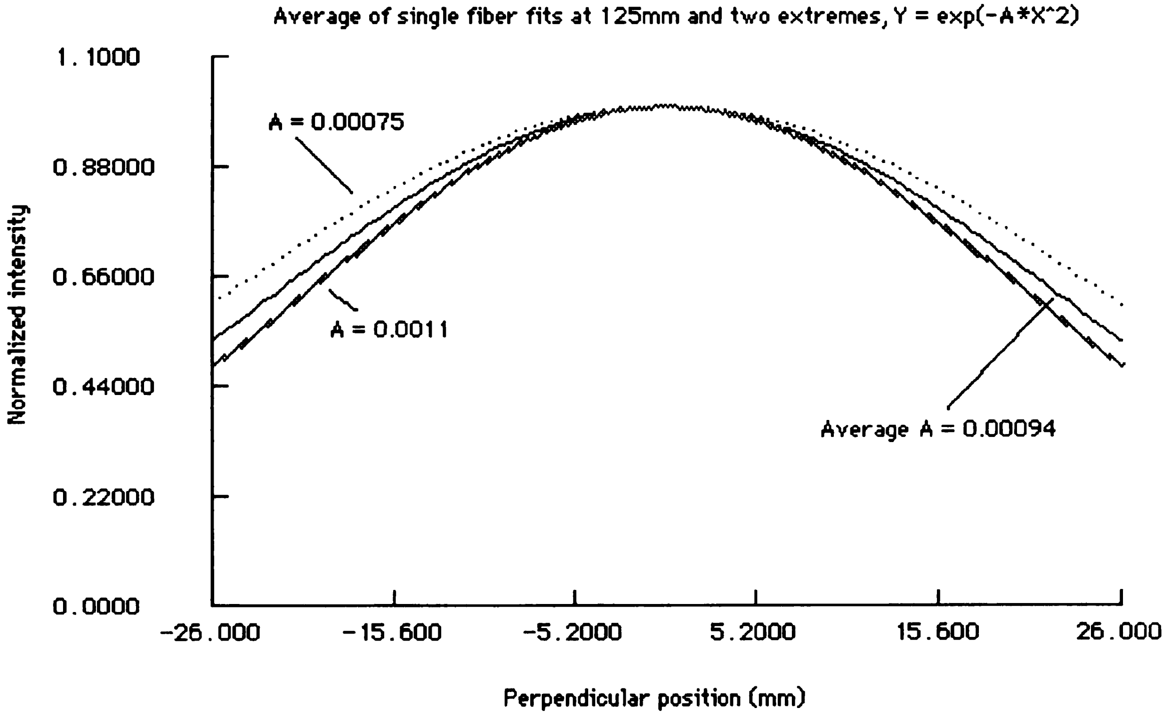

Figure 5.2: One parameter Gaussian fit to the light output from a single fiber. Plotted are the average and two extremes fits at 125mm from the fiber face. Values given are for the generic fit parameter.

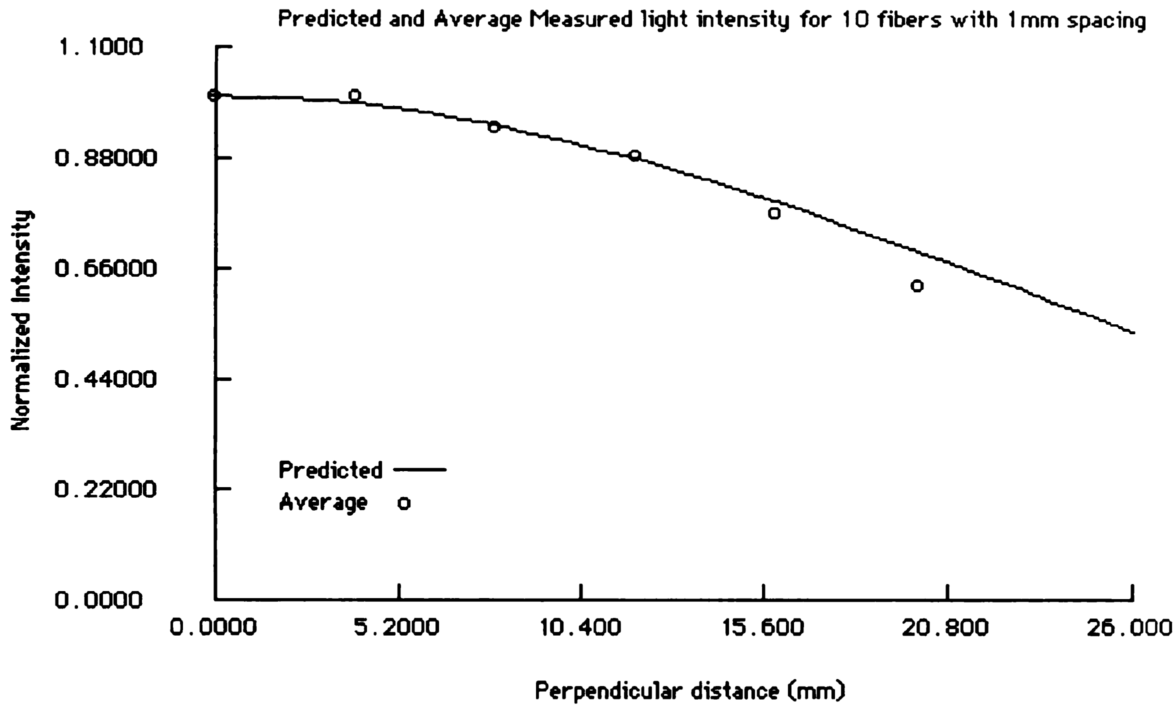

Figure 5.3: Average measured and predicted light intensity from a linear array of ten fibers spaced 1.0mm apart. The predicted curve is based on the Gaussian model for the light distribution from a single fiber.

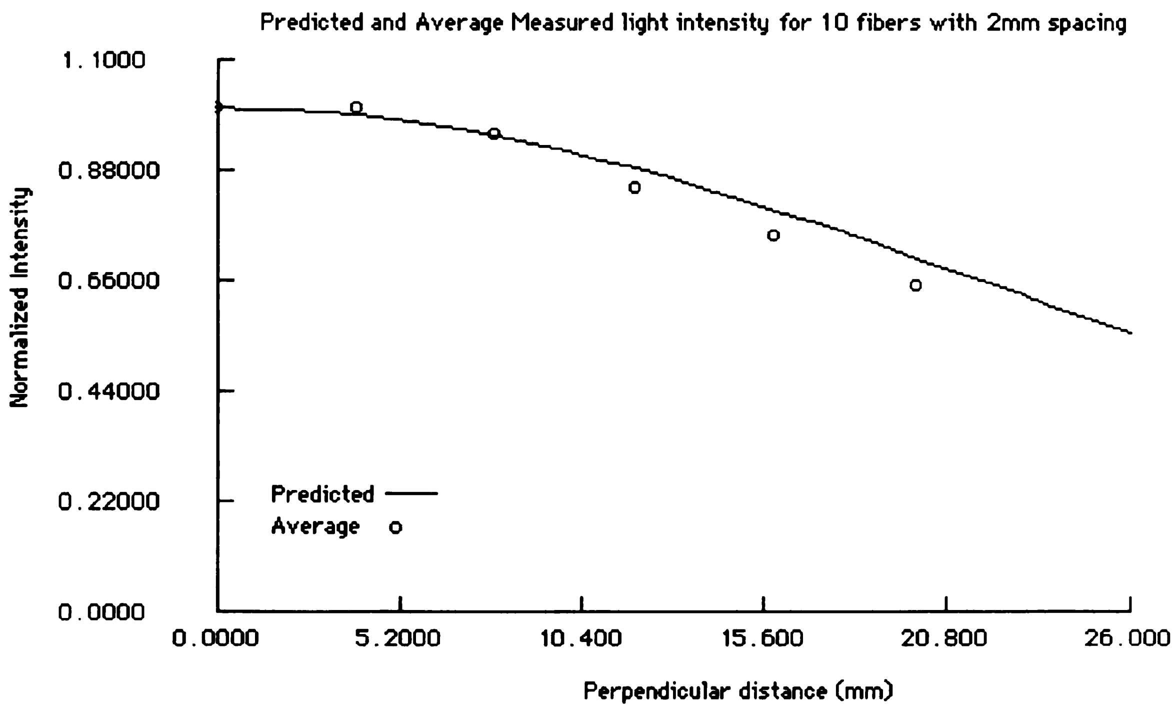

Figure 5.4: Average measured and predicted light intensity from a linear array of ten fibers spaced 2.0mm apart. The predicted curve is based on the Gaussian model for the light distribution from a single fiber.

Table 5.1: Percent difference between normalized data from a linear array of 10 fibers with a 1.0mm center-to-center spacing and normalized data generated using the Gaussian model for the light output from a single fiber. Each number represents a cell where actual data was measured. Negative numbers indicate that the simulated value exceeded the actual value measured for that cell.

-15.7	-14.4	-12.0	-8.6	-12.6	-4.3	-12.6	-8.6	-12.0	-14.4	-15.7
-26.7	-25.5	-12.6	-10.8	-5.7	1.5	2.9	-1.9	-2.9	-4.2	-2.2
-12.0	-12.6	-4.5	-3.4	-0.2	-1.4	-0.2	4.6	4.2	-2.9	-1.0
-7.2	-10.8	-3.4	-2.5	0.4	-1.7	0.4	5.0	-3.4	-1.9	-7.2
-11.3	-5.7	0.9	0.4	3.1	1.0	3.1	0.4	0.9	-5.7	-1.5
-12.6	-6.9	-1.4	-0.6	1.0	0.0	1.0	-0.6	-1.4	1.5	-2.9
-11.3	-5.7	-6.8	0.4	3.1	1.0	3.1	0.4	0.9	-5.7	-1.5
-7.2	-10.8	-3.4	-2.5	0.4	-1.7	0.4	-2.5	-3.4	-1.9	-7.2
-12.0	-12.6	-13.2	-11.5	-7.9	-1.4	-0.2	-3.4	-4.5	-2.9	-12.0
-14.4	-14.8	-12.6	-10.8	-5.7	-6.9	-5.7	-10.8	-2.9	-14.8	-14.4
-15.7	-14.4	-12.0	-8.6	-12.6	-13.9	-12.6	-8.6	-12.0	-14.4	-15.7

Table 5.2: Percent difference between normalized data from a linear array of 10 fibers with a 2.0mm center-to-center spacing and normalized data generated using the Gaussian model for the light output from a single fiber. Each number represents a cell where actual data was measured. Negative numbers indicate that the simulated value exceeded the actual value measured for that cell.

-8.5	-10.7	-11.9	-11.0	-9.1	-15.1	-14.1	-16.0	-16.9	-15.7	-13.5
-9.6	-7.9	-10.1	-10.3	-8.4	-9.4	-8.4	-10.3	-10.1	-7.9	-9.6
-0.8	-4.1	-2.3	-2.5	-1.6	-2.6	-1.6	-7.5	-7.3	-9.1	-10.8
-4.9	-9.2	-7.5	-3.7	-2.8	0.2	2.2	1.3	-2.5	0.8	-4.9
-8.0	-7.3	-6.6	-2.8	-1.9	-4.0	-1.9	-2.8	-1.6	-2.3	-3.0
-4.1	-3.4	-2.6	-3.8	-4.0	0.0	1.0	1.2	-2.6	-3.4	-4.1
-8.0	-7.3	-1.6	-2.8	-1.9	1.0	3.1	2.2	-1.6	-2.3	-3.0
-4.9	-4.2	-2.5	-3.7	2.2	0.2	2.2	-3.7	-2.5	-4.2	-4.9
-5.8	-4.1	-2.3	-2.5	-1.6	-2.6	-1.6	-2.5	-2.3	-4.1	-5.8
-4.6	-7.9	-5.1	-5.3	-3.4	-4.4	-3.4	-5.3	-5.1	-7.9	-4.6
-8.5	-10.7	-6.9	-6.0	-9.1	-5.1	-9.1	-6.0	-6.9	-5.7	-8.5

Table 5.3: The cell-by-cell percent difference between the normalized light output from the 1.0mm bundle and the normalized simulated data for three linear arrays of fibers. A negative value indicates that the simulated data exceeds the actual data for that cell. The "–" in the first column is an artifact of the matching of the two data sets.

–	-23.1	-23.4	-22.0	-20.7	-20.1	-20.7	-19.8	-20.9	-23.1	-21.1
–	-20.7	-17.6	-15.5	-13.4	-12.9	-11.4	-13.5	-15.4	-18.3	-19.9
–	-15.4	-12.2	-9.2	-6.5	-5.9	-6.5	-7.4	-10.3	-13.2	-15.5
–	-15.5	-9.2	-7.3	-4.9	-3.1	-1.7	-2.3	-3.8	-7.4	-12.4
–	-11.4	-6.2	-3.3	-1.5	-1.3	0.0	1.5	0.8	-1.8	-4.8
–	-6.9	-2.5	0.1	0.2	0.0	1.7	1.7	2.6	-1.2	-4.1
–	-5.7	-2.7	1.5	1.6	1.7	3.1	4.7	4.2	2.0	-0.4
–	-3.4	-0.2	2.8	3.1	4.8	4.7	4.5	5.3	2.6	-3.2
–	-6.7	-2.5	1.7	3.8	6.1	5.6	5.3	3.4	-0.2	-3.1
–	-8.6	-4.5	0.6	2.0	4.1	4.0	2.6	2.0	-1.4	-3.3
–	-6.7	-6.1	-3.7	-3.1	-2.8	-3.1	-3.7	-6.1	-9.4	-11.7

Table 5.4: The cell-by-cell percent difference between the normalized light output from the 2mm bundle and the normalized simulated data for three linear arrays of fibers. Negative indicates that the simulated data exceeds the actual data for that cell. The "–" in the first column is an artifact of the matching of the two data sets.

–	-17.1	-13.5	-12.0	-9.4	-7.7	-9.0	-7.7	-9.4	-8.8	-10.0
–	-19.7	-17.1	-13.9	-9.5	-8.4	-7.5	-5.9	-6.9	-5.2	-7.6
–	-11.0	-10.5	-6.4	-3.7	-1.0	2.0	1.3	1.1	1.4	-1.9
–	-11.0	-8.7	-3.3	-1.1	1.0	1.6	1.0	1.2	-1.0	-3.3
–	-11.7	-7.2	-2.6	-1.2	0.8	1.4	0.8	1.0	2.1	0.5
–	-10.1	-5.9	-1.8	-0.1	-0.6	0.0	1.4	2.0	0.5	1.8
–	-11.7	-9.8	-4.9	-1.2	-1.3	-0.6	0.8	1.0	2.1	0.5
–	-11.0	-8.7	-5.8	-1.1	1.0	1.6	3.1	3.4	1.5	2.0
–	-17.6	-13.4	-11.6	-6.1	-3.3	-2.6	-1.0	-1.3	-1.2	-4.8
–	-23.4	-20.3	-16.7	-14.9	-11.0	-7.5	-5.9	-6.9	-5.2	-7.6
–	-25.4	-20.7	-18.5	-18.4	-16.3	-14.7	-13.4	-12.4	-12.0	-13.5

Table 5.5: Percent difference between the normalized light output from the 1.0mm bundle and the normalized sum of the individual linear arrays from which the bundle is made.

–	11.4	8.0	5.3	3.8	-0.2	-6.0	-5.6	-7.8	-10.0	-9.1
–	19.9	13.4	9.7	7.5	3.9	-1.4	-5.4	-6.9	-11.2	-16.4
–	16.4	10.6	10.0	7.5	4.5	-1.9	-7.3	-12.6	-14.3	-18.8
–	9.7	12.9	9.5	4.9	2.0	2.0	-4.9	-5.7	-12.6	-16.4
–	9.9	10.1	6.7	2.9	0.6	0.6	-0.6	-4.9	-7.3	-12.3
–	13.8	13.4	9.7	4.1	0.0	0.0	-2.7	-5.4	-11.3	-14.5
–	13.8	14.2	9.7	2.2	0.0	0.0	-1.2	-3.6	-3.7	-10.4
–	18.0	14.9	13.3	7.0	4.1	0.6	-2.2	-4.9	-7.3	-12.2
–	15.9	16.1	17.0	11.4	5.8	4.1	1.0	0.7	-6.2	-6.9
–	22.2	18.6	19.4	13.6	12.1	7.5	4.0	0.7	-2.1	-5.6
–	23.6	22.2	21.0	18.6	14.0	11.4	6.4	2.5	-1.5	-6.4

Table 5.6: Percent difference between the normalized light output from the 2.0mm bundle and the normalized sum of the individual linear arrays from which the bundle is made.

22.1	26.5	36.2	33.8	37.5	42.8	42.8	45.0	47.6	52.6	–
16.0	16.0	20.0	23.2	22.8	22.6	26.2	23.0	27.6	24.6	–
16.0	16.0	16.0	19.0	18.8	21.4	18.7	21.8	22.3	27.2	–
8.5	16.0	16.0	13.4	13.6	9.2	9.0	8.8	10.6	7.1	–
5.5	7.1	10.7	6.7	5.3	5.5	3.3	4.8	6.3	5.2	–
-0.1	2.2	3.9	4.8	3.3	1.8	1.8	1.2	0.1	3.1	–
-0.6	-1.0	-2.9	0.7	-0.6	-2.0	-2.0	-2.6	-1.8	-1.7	–
-3.9	-3.8	-5.8	-1.8	-2.6	-2.3	-2.3	-1.2	-4.5	-4.2	–
-12.1	-13.0	-14.3	-11.3	-9.8	-9.3	-9.3	-10.3	-10.0	-13.0	–
-23.9	-21.6	-19.9	-21.0	-18.8	-15.8	-15.8	-17.1	-13.0	-13.7	–
-22.7	-14.9	-19.4	-21.7	-21.8	-22.7	-20.9	-21.8	-19.7	-18.1	–

Table 5.7: Percent difference between the light output from the 1.0mm bundle and the sum of the individual linear arrays from which the bundle is made.

27.3	19.2	13.3	5.9	2.8	-7.7	-10.3	-17.9	-22.2	-21.9	-25.0
37.5	31.0	23.5	15.4	7.0	-2.1	-10.4	-17.0	-20.9	-25.6	-28.6
34.5	32.4	22.0	14.9	7.8	0.0	-7.3	-14.8	-23.1	-27.7	-31.7
31.2	31.6	22.2	15.7	8.9	5.2	-1.7	-10.2	-16.4	-24.0	-27.3
39.4	38.5	27.7	18.5	8.3	4.8	1.6	-4.9	-12.1	-18.9	-25.5
48.5	46.2	37.0	24.5	15.5	11.7	6.7	3.4	-7.1	-15.4	-23.9
53.1	47.4	43.2	29.4	19.6	13.6	10.2	3.4	-3.6	-10.0	-20.0
54.8	52.8	41.9	33.3	24.5	16.1	10.7	5.5	-1.9	-10.6	-17.1
53.6	51.5	47.4	39.5	29.2	19.6	13.7	6.0	0.0	-7.1	-11.1
46.2	51.7	47.1	35.9	31.0	22.7	13.3	9.3	0.0	-2.8	-9.4
61.9	52.0	44.8	37.5	32.4	25.7	16.7	8.6	0.0	-6.7	-14.8

Table 5.8: Percent difference between the light output from the 2.0mm bundle and the sum of the individual linear arrays from which the bundle is made.

-10.5	-9.1	4.3	3.8	11.1	23.1	23.1	33.3	36.4	47.4	47.1
-13.6	-15.4	-10.3	-6.2	0.0	2.9	8.8	12.1	16.7	22.2	31.8
-18.5	-12.9	-13.9	-7.7	-4.8	0.0	4.7	10.0	13.5	25.8	25.9
-22.6	-14.7	-15.0	-11.1	-8.3	-7.8	-4.0	-2.1	4.7	5.1	12.5
-24.2	-23.1	-18.2	-16.0	-14.8	-10.9	-9.1	-5.8	-2.1	2.3	8.3
-30.6	-26.2	-22.9	-17.3	-14.5	-14.0	-12.3	-9.1	-5.9	-2.2	5.3
-28.6	-26.8	-28.6	-22.6	-17.9	-17.2	-15.5	-12.5	-9.6	-4.3	-2.5
-34.3	-29.3	-29.2	-25.0	-21.4	-17.5	-15.8	-11.1	-9.8	-8.7	-5.0
-36.4	-37.5	-34.8	-33.3	-27.8	-23.6	-21.8	-18.9	-16.3	-13.6	-10.8
-43.8	-43.2	-40.5	-38.3	-36.0	-31.4	-27.5	-24.5	-20.5	-15.4	-14.7
-40.7	-40.0	-38.9	-37.5	-37.2	-35.6	-31.8	-30.2	-25.6	-20.6	-17.2

Chapter 6

Potential Application: A Fiber Based Headlight System

The use of fiber optics for non-imaging illumination tasks was the focus of this thesis, with use in an automotive headlight system the primary example. We will now examine this potential application in more detail.

6.1 Advantages of Fiber Optics Headlights

There are several advantages to using a fiber optic based system as compared with a traditional headlight. Existing headlights are composed of a standard filament bulb in combination with a complex multi-segmented mirror and a lens/mask array to selectively focus or mask the light in order to create the required headlight pattern. A fiber based system (or central lighting system) would consist of a single source for the headlights (different sources could be used for other lighting systems in the car) leading into a main fiber which in turn branches into each headlight. The fiber would be further branched and set in position; addition of a much less complex mirror, if any, and a few relatively simple lenses would complete the system. Figure 6.1 shows an idealized layout of a fiber system as compared to the current system.

The current technology is weak in several areas. For each conventional headlight

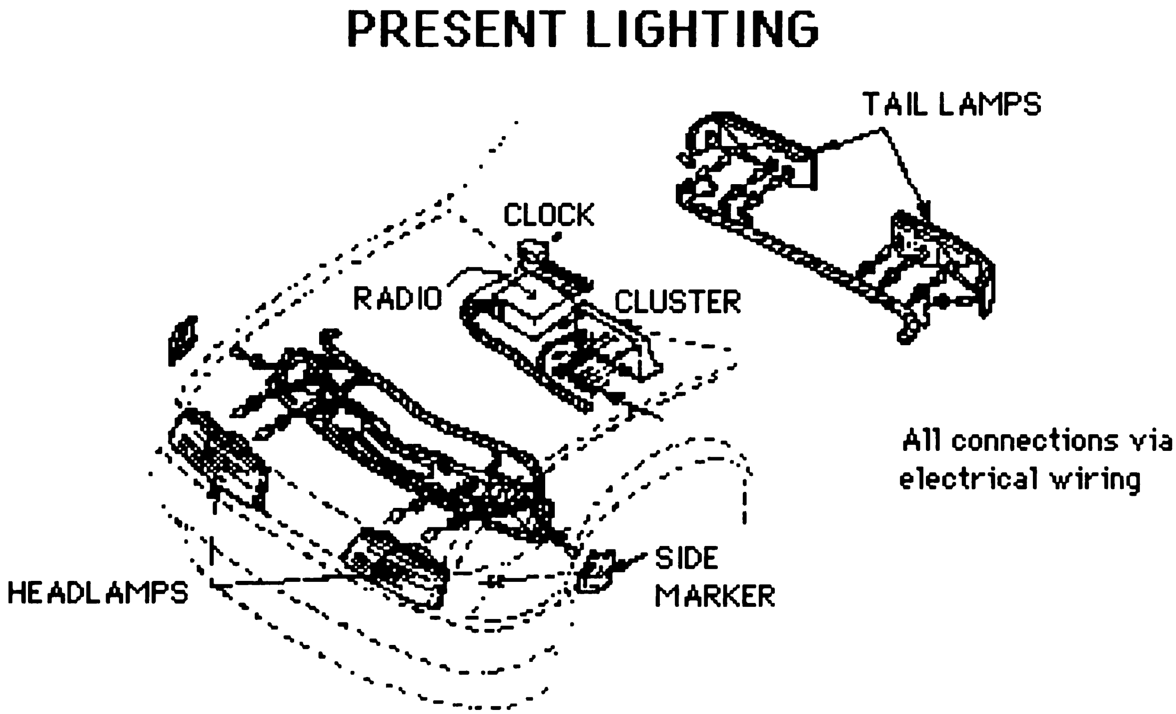

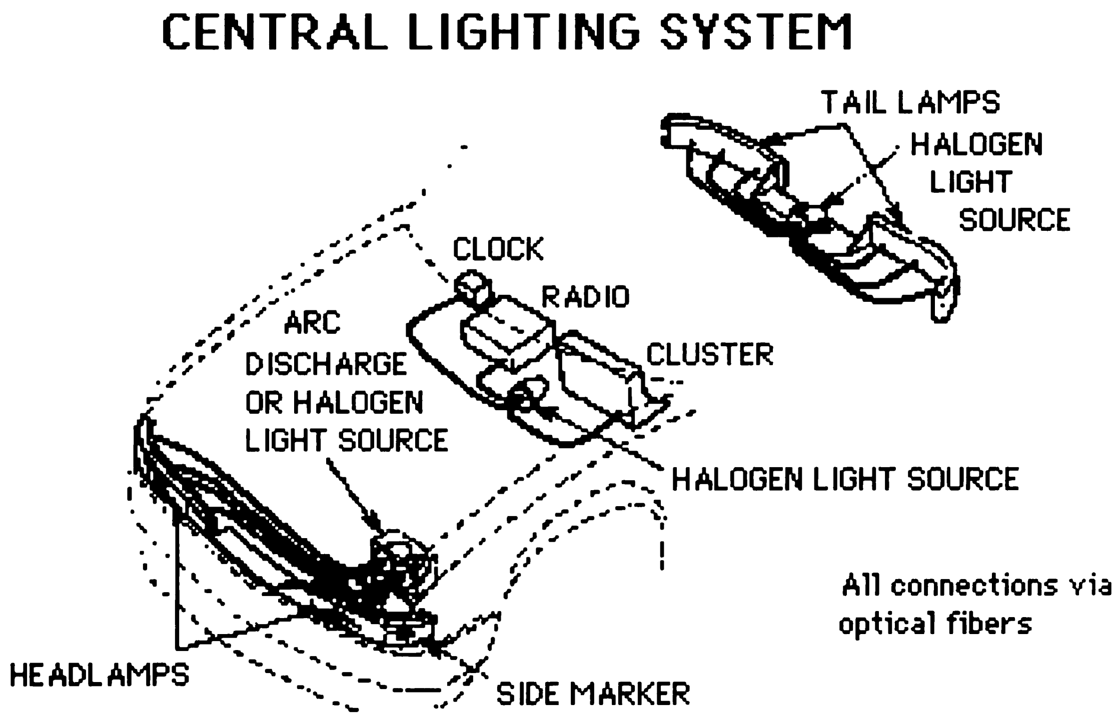

Figure 6.1: A comparison of the existing lighting system in most cars (top) to a fiber based central lighting system (bottom). Note the large reduction in the number of individual sources needed to achieve the same goal [Ford9].

three bulbs are needed: one for the low beam, one for the high beam and one for the side light. This is a redundancy that a fiber based system would eliminate by using only one source to replace all the bulbs in both headlights. This single source would be isolated from the headlights allowing for easy service. When a present bulb fails, the entire headlight including the mirror and lens array (which are completely intact) must be replaced. In a fiber based system, should the source fail it need only be replaced from inside the engine compartment, without disturbing the headlight itself. Also, if the light source contains a secondary source it could still illuminate both headlights in the event that the primary source fails, causing nothing more than perhaps a dimming of both headlights instead of the complete failure of one. This adds a measure of safety that would not be easily implemented in a traditional arrangement. The car with one headlight that is often mistaken for a motorcycle would become a thing of the past. In addition, there would be fewer replacements of the single source and virtually no need to maintain the fiber system itself. The fibers would be fixed during manufacture thereby eliminating the misalignment which often results when replacing a traditional headlight. The cost of a single replacement source would eventually be less than the replacement cost of a present headlight. This nearly "maintainance-free" system would have a longer lifespan than present headlights as well [Ford10].

Existing headlights are inefficient, with a 40% efficiency on average [Ford11]. An optical fiber can transport high intensities of light very efficiently, with typical dealer catalog values of up to 90% for a fiber bundle. This high efficiency would allow for a reduced intensity (i.e. lower power) source to be used to generate the same amount of light as a traditional headlight.

A fiber based system would undoubtedly be less complex to design and build than current headlights. It takes considerable effort, trial and error, and patience to design a headlight. The mirror must be such that it will transform the spherical light waves emitted by the bulb into an essentially parallel beam of light which, when passed through the front lens array, will generate the desired pattern on the road. In this process much light is lost and by necessity the headlight as a whole must be large compared to the size of the bulb filament. A fiber's light output is highly directional and would therefore require a smaller, less sophisticated mirror to achieve the same end. This new freedom in the size of the headlight would be welcomed by automotive design teams and could lead to dramatic, new front end styles in cars to come.

6.2 Physical Characteristics

The physical realization of the ideal of Figure 6.1 is, of course, a goal beyond the limits of this thesis. At present, only some of the more important characteristics of a fiber based lighting system can be discussed.

The light from the source would need to be transported to the headlights via a large fiber on the order of .25 to .5 inches in diameter. This fiber would likely be made of some type of plastic that would be resistant to the many substances that are found inside the engine compartment, namely, road salt, water, gasoline, oil, various cleaners and degreasers, alcohol, paint, etc. The large fiber will run directly into the headlight itself where it would branch into relatively few (approximately 10 or so) smaller diameter fibers which would in turn be mounted in place to build the headlight pattern. The pattern could be built of the fibers themselves or from a clear plastic mold that would distribute the light from the fibers. A possible shape for this mold is shown in Figure 6.2.

This mold would allow the input fiber to be attatched at the side to facilitate design, i.e. the primary fiber can be run along the outside edge of the engine com-

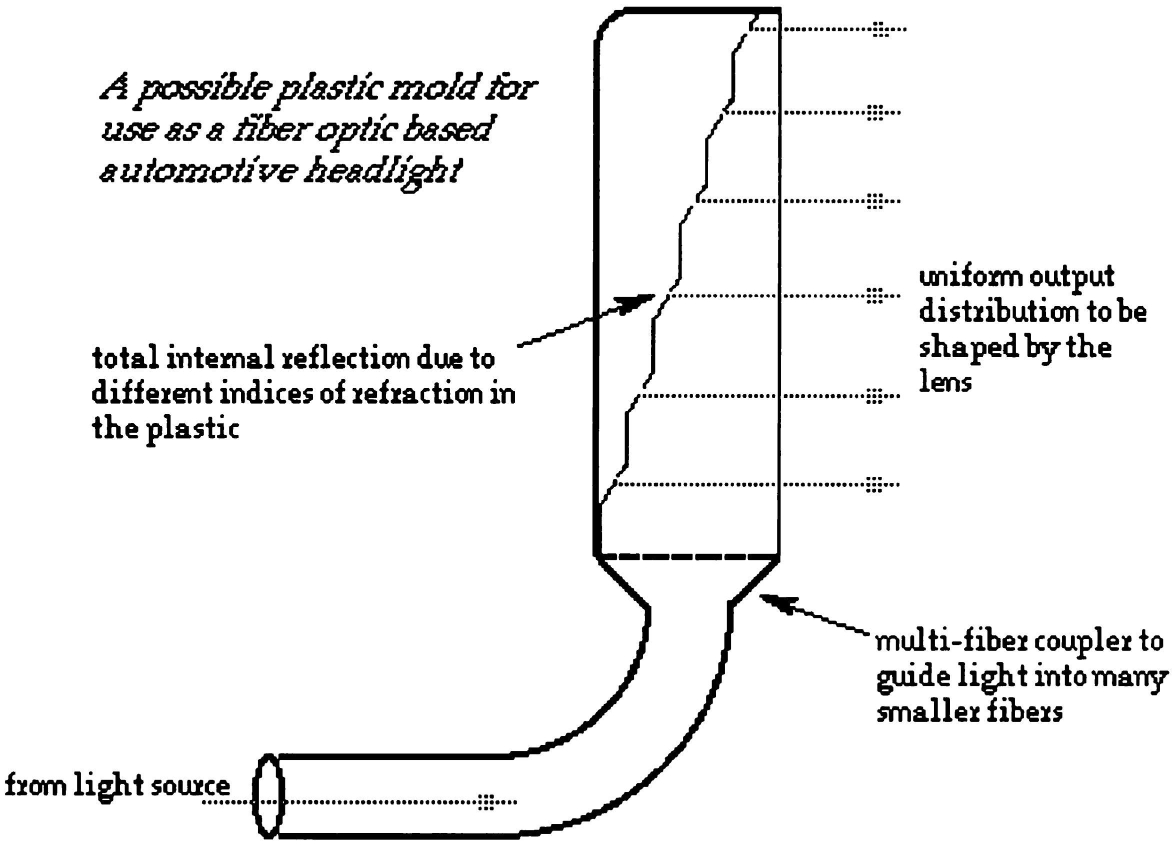

Figure 6.2: A clear plastic mold with the proper shape could be used to generate the headlight pattern when fed by light from the optical fibers. A possible shape is shown, the light from the fibers would be reflected as indicated. The majority of the headlight pattern could be built before the lens, a radical departure from the traditional approach [Ford12].

partment, not the middle. This particular design removes the need for a mirror as all of the reflection is performed internally by the plastic, thereby reducing production costs. If the input fibers are arranged linearly the output from the mold will be very uniform and easily manipulated by a much less sophisticated lens and mask system than is in present use.

6.3 Requirements of an Automotive Headlight

A properly aimed low beam headlight will project an oblong pattern with the brightest spot at a position that is in the fourth quadrant of the axes formed with the center of the headlight at the origin, as illustrated in Figure 6.3.

This light pattern is easily generated by a linear array of fibers and a cylindrical lens. Table 4.6 demonstrates the rapid decrease in light intensity in the vertical as compared to the horizontal.

6.4 Areas for Future Research

There exist several areas where extensive further research is required. Among them are: (1) the light source, (2) manifolding of the fibers, (3) the necessary lenses, and (4) the fiber arrays. The first two areas were not addressed in this paper and only general comments will be made for each. The light source for a fiber based headlight system would be safely enclosed within the engine cavity and separated from the headlights themselves. An arc discharge lamp would be a likely candidate for suitable light source [Sentinel14].

The manifolding of the fibers from the primary fiber (from the light source) to the many smaller fibers that will be used to build the headlight is an area of concern. An efficient system must be found in order to take advantage of the fiber's ability to

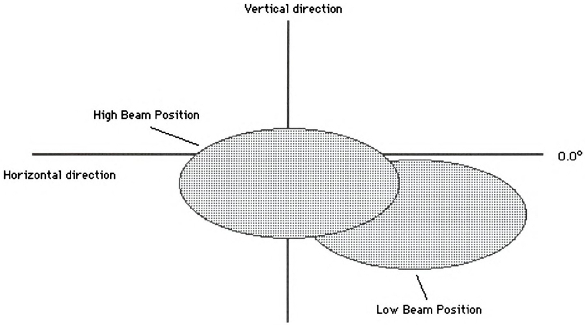

Figure 6.3: Position of the projected light from an automotive headlight as projected onto a screen 25 feet from the vehicle. The origin is at the same height as the center of the headlight. Notice that the light from the low beam is confined to the fourth quadrant and does not project above the headlights themselves. This oval pattern is easily produced by a linear array of fibers and a cylindrical lens. Image re-drawn from [Time13].

transmit highly concentrated amounts of light with low loss.

The final two areas will be discussed together. From the results of this research it is evident that a linear array of fibers is an appropriate building block for a functional headlight. Examination of the light patterns generated from a linear array of fibers, especially in conjunction with a cylindrical lens, shows that such a combination has the necessary symmetry and shape to be consistent with federal requirements for a low beam headlight. This is in high contrast to the comparatively extensive manipulation of the essentially spherical radiation pattern generated by a conventional filament bulb to create an acceptable headlight. Further research will be needed to determine the number and orientation of these basic building "blocks" in order to create a headlight suited to the vehicle under consideration.

Appendix A

Fiber Transmission Efficiency as a Function of Wavelength

The transmission efficiency of the 6.0mm diameter fiber on the incident light as a function of wavelength was tested against that of a 3.0mm bundle of glass fibers. The setup used for this test is shown in Figure A.1. The filter was adjustable from $4000\AA$ to $7000\AA$. Data was taken at $200\AA$ intervals.

The absolute output power in milliwatts was measured and plotted against the actual power incident from the lamp alone. This is shown in Figure A.2. Figure A.3 shows the glass bundle and plastic fiber alone. Notice how well the glass bundle preserves the original form of the incident light, and how much the plastic fiber changes it. This would be an important consideration in an automotive headlight. Since glass fibers would not be used in such a system (they are too fragile and expensive) there are two choices left: find a suitable plastic (i.e. one that preserves the functional form) or alter the source to make up for the deficiencies in the plastic. The former will likely be the method chosen. One can even imagine selecting a plastic so that it will tailor the color of the headlight to something other than white, perhaps orange to reduce the glare and improve visibility.

Figure A.4 is derived from Figure A.2 and shows more clearly the effects of the

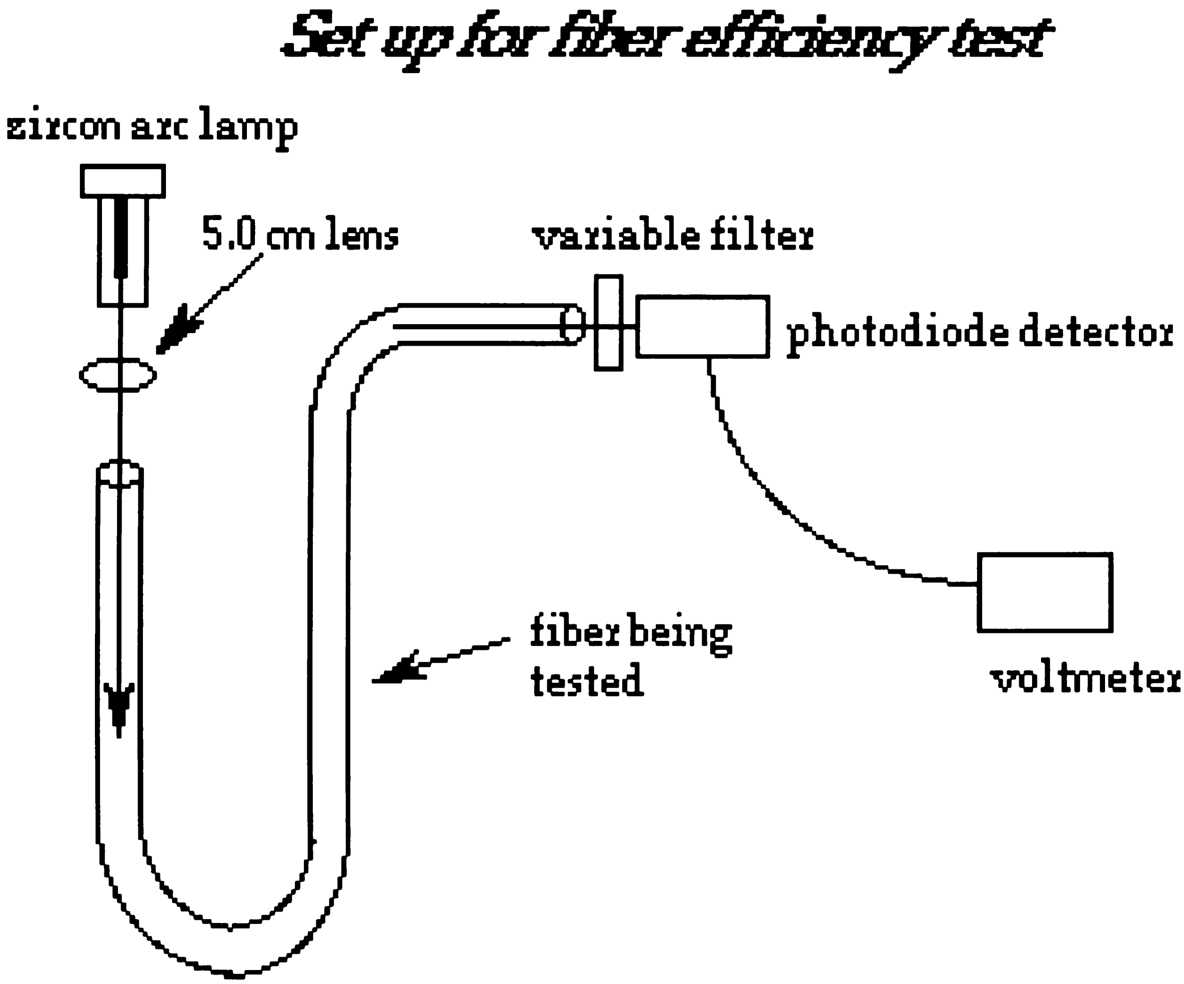

Figure A.1: Set up used in fiber efficiency testing. Note, bending in the figure is for display purposes only, actual fibers were set up without bending.

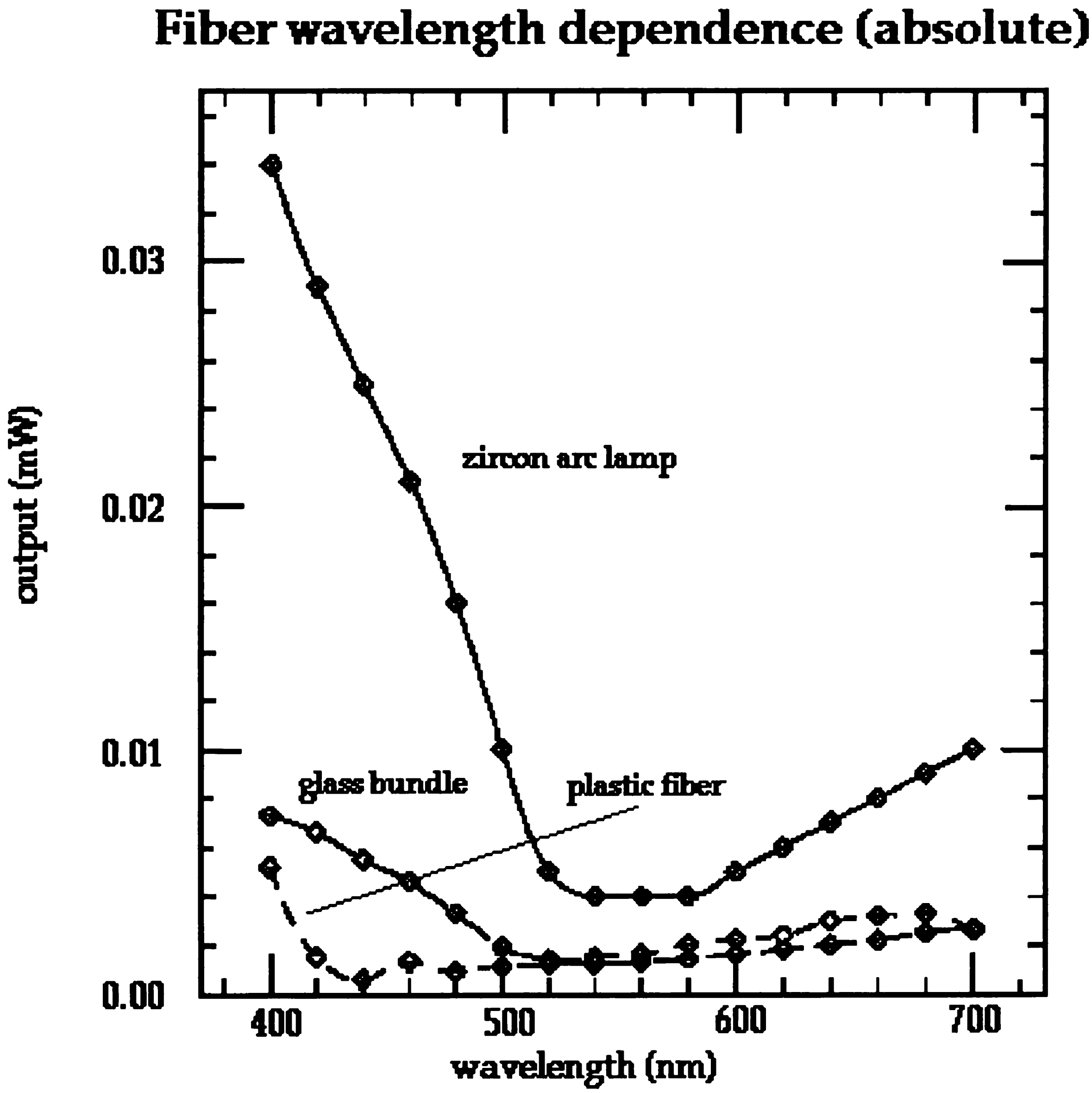

Figure A.2: The absolute power per wavelength transmitted by the 6.0mm plastic fiber and 3.0mm glass bundle compared to the original output power of the Zr lamp. Note functional form of the glass bundle and Zr lamp.

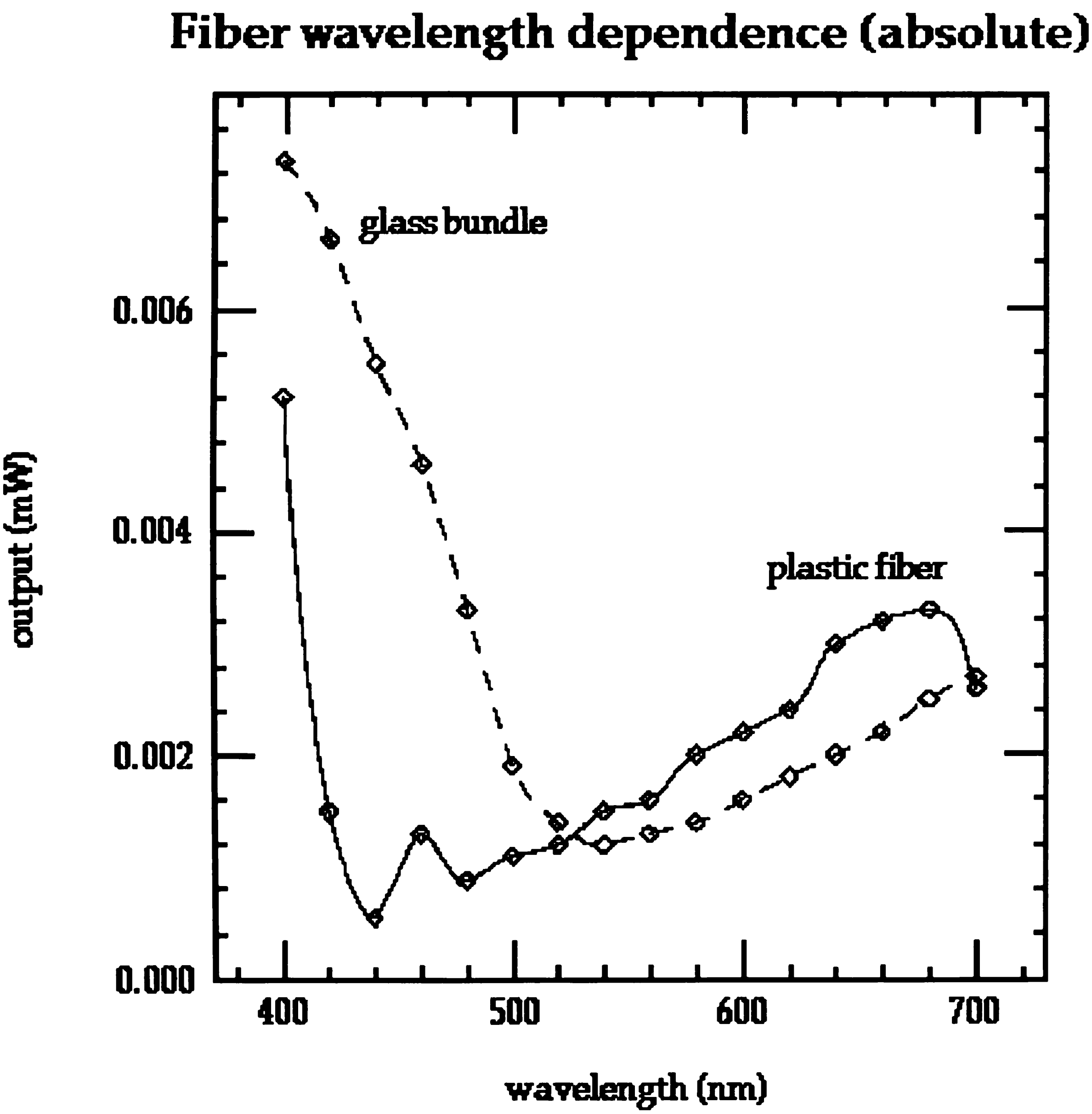

Figure A.3: Close up of Figure A.2 showing the glass bundle and plastic fiber more clearly. Notice how similar in functional form the glass bundle is to the Zr source lamp.

plastic and glass on the incident light. The glass bundle is tending towards a uniform transmission over the visible while the plastic exhibits great variation, from a low of 2% at 4400$\AA$ up to 50% at 5800$\AA$.

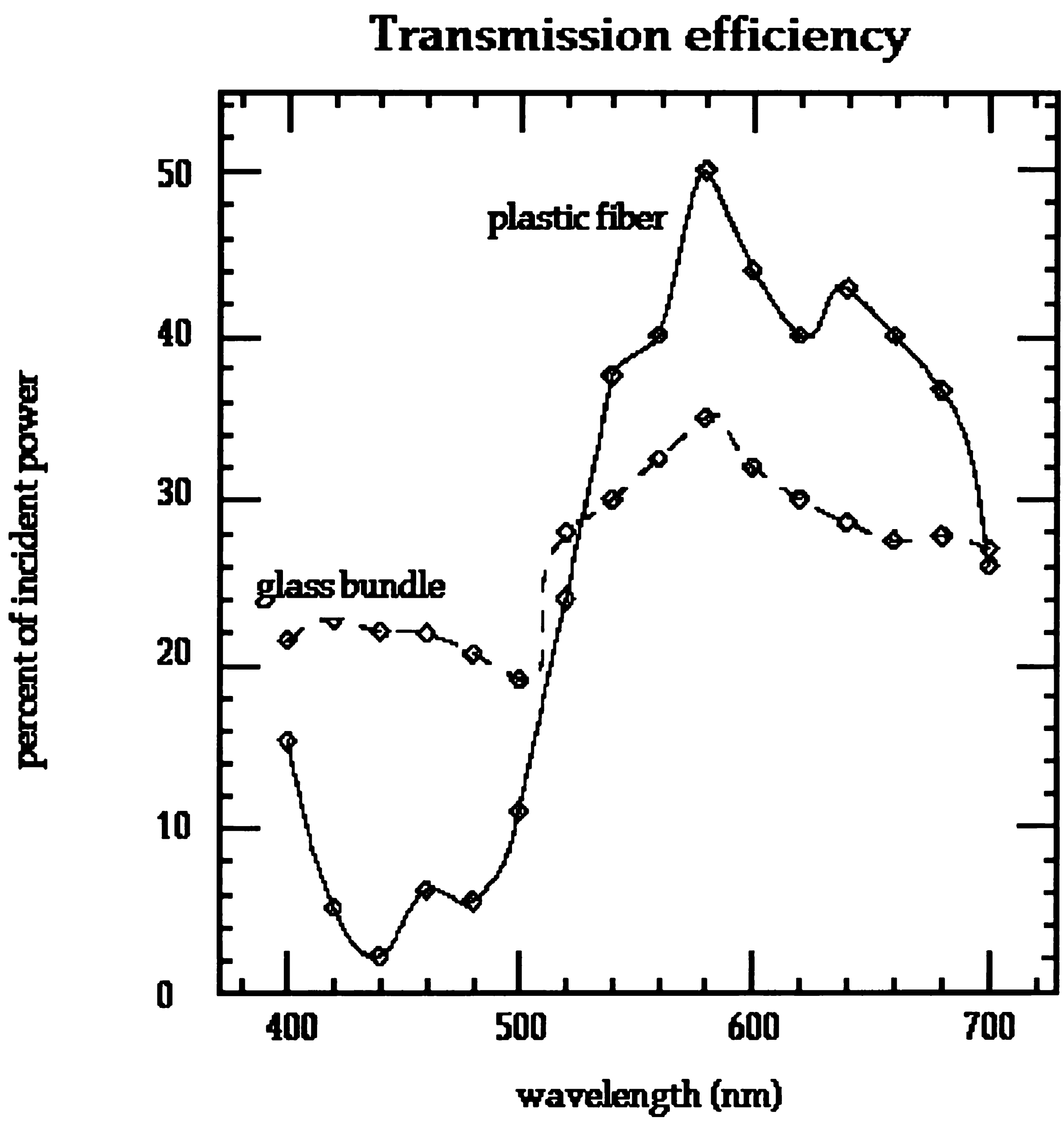

Figure A.4: The percent of incident light transmitted per wavelength for the plastic fiber and glass bundle. Notice the wide variation in the plastic's transmission efficiency and the more uniform transmission of the glass bundle.

Appendix B

Detector Calibration

The photovoltaic detector used in this experiment was calibrated relative to a known power meter (*Newport Research Corporation laser power meter model 820* or *NRC*). The light source used during the calibration was a standard laboratory helium-neon gas laser ($\lambda = 6328\mathring{A}$). Variation in laser intensity was achieved by placing neutral density filters or combinations thereof between the laser and the detector. This allowed for several orders of magnitude change in the incident beam intensity. Several measurements were made over a wide range of intensities, the results of which are given in Table B.1.

Figure B.1 shows a typical fit for the calibration data. From the table it is evident that the detector can be used to measure directly in milliwatts to within 8% for

Table B.1: Results of photovoltaic detector calibration.

Power range (mW)		Best fit	
low	*high*	*slope(V/mW)*	*intercept(V)*
0.01	1.15	0.9175 ± 0.0006	$1.25 \times 10^{-4} \pm 1.0 \times 10^{-5}$
0.01	1.15	0.9214 ± 0.0006	$-3.3 \times 10^{-5} \pm 1.0 \times 10^{-5}$
0.0001	0.005	0.936 ± 0.005	$-1.3 \times 10^{-5} \pm 5 \times 10^{-6}$

Average	0.9250 ± 0.0017 V/mW

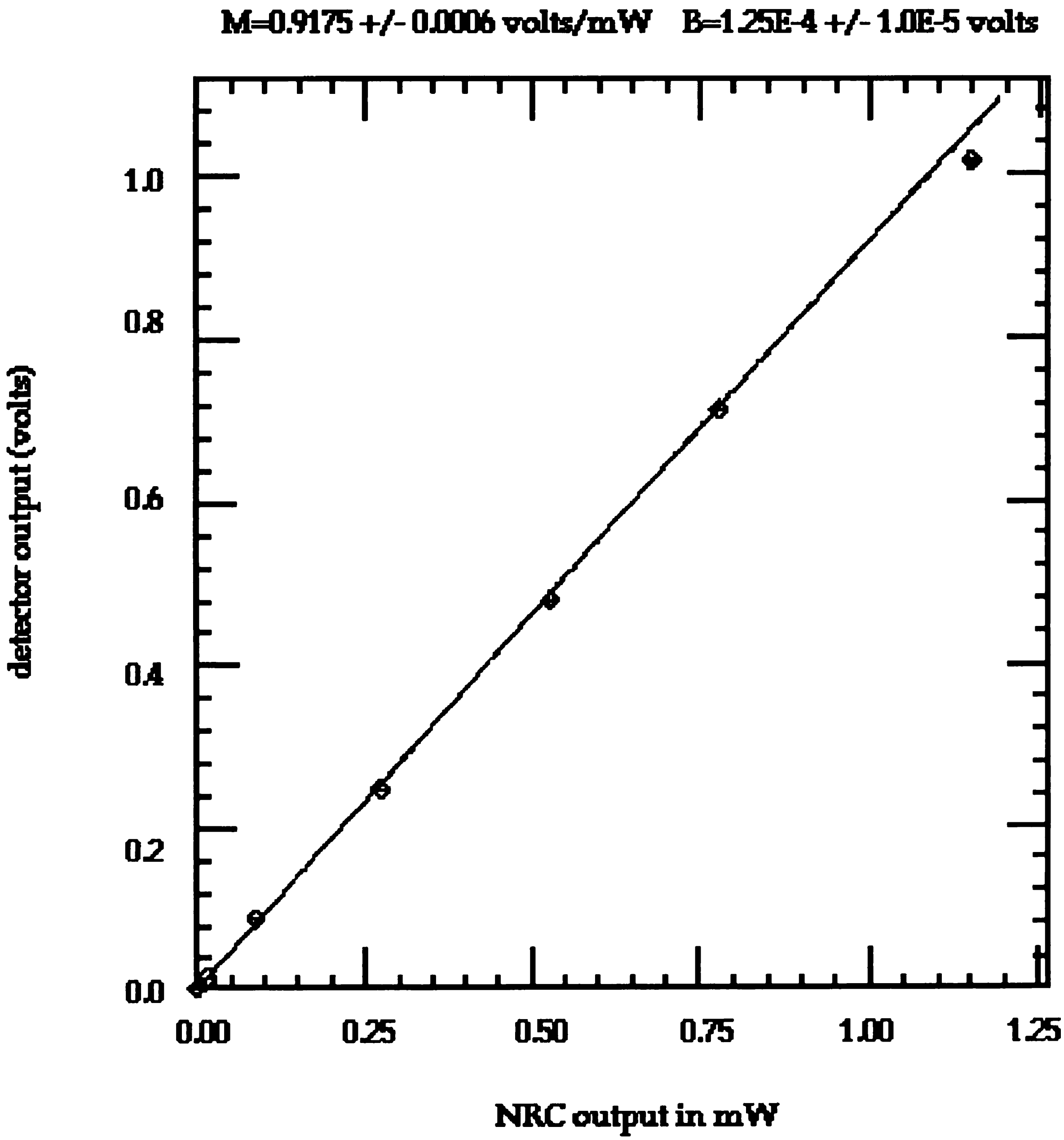

Figure B.1: A typical fit for the photovoltaic detector calibration.

intensities below 1.0mW. Intensities above 1.0mW will cause the detector to operate in the saturation region where the response is no longer linear.

Appendix C

Program Listings

A listing of some of the more important computer programs written for this thesis is now presented. The programs listed were written in the Pascal programming language for the Apple Macintosh.

C.1 Program 1. Simulate the Light Distribution of a Linear Fiber Array in 2 Dimensions

Pascal Program 1 was used to simulate the 2-dimensional light output of a linear array of fibers with a 1mm or 2mm center-to-center spacing at a distance of 125mm from the array. It is based on the generic Gaussian (one parameter) model. A variation of this program was used to simulate the light distribution from three linear arrays stacked one on top of the other.

```
program twodImage;

{ Generates an 11x11 file of reals representing the  }
{ intensity for a 2d image at 125mm from the face of }
{ an array of 10 fibers with either a 1mm or 2mm spacing. }

{  RTK, 06-16-93, for thesis. }

const
a = 0.00093925;  {  generic fit constant for 125mm }

type
```

```
offsetsType = array[1..10] of real;
imageType = array[1..11, 1..11] of real;

var
f: text;
i: integer;
xi: offsetsType;
image: imageType;

procedure fill1mm (var xi: offsetsType);
begin
xi[1] := -4.5;     { Offsets to center Gaussian }
xi[2] := -3.5;     { around a particular fiber  }
xi[3] := -2.5;
xi[4] := -1.5;     { for 1mm spacing }
xi[5] := -0.5;
xi[6] := 0.5;
xi[7] := 1.5;
xi[8] := 2.5;
xi[9] := 3.5;
xi[10] := 4.5;
end;

procedure fill2mm (var xi: offsetsType);
begin
xi[1] := -9.0;     { Offsets for 2mm spacing }
xi[2] := -7.0;
xi[3] := -5.0;
xi[4] := -3.0;
xi[5] := -1.0;
xi[6] := 1.0;
xi[7] := 3.0;
xi[8] := 5.0;
xi[9] := 7.0;
xi[10] := 9.0;
end;

function z (x, y: real; n: integer): real;
begin
z := exp(-a * ((x - xi[n]) * (x - xi[n]) + y * y));
{ function to calculate the intensity at the point }
{ (x,y) which is 125mm way from the array }
end;

procedure zeroimage (var image: imageType);
var
  i, j: integer;
begin
  for i := 1 to 11 do       { zero image array }
for j := 1 to 11 do
```

```
  image[i, j] := 0.0
end;

function fn (b: real): integer; { converts fiber number }
begin                           { into a true position }
fn := (20 - trunc(b)) div 4 + 1
end; { of fn }

procedure MakeImage (var image: imageType);
var
x, y: real;
i: integer;
begin                           { creates the image by summing }
  for i := 1 to 10 do           { the intensities produced at  }
begin                       { each point for each fiber in }
  x := -20.0;               { the array.                   }
  write(i : 2, ' ');
  while (x <= 20) do
begin
  y := -20.0;
  while (y <= 20) do
    begin
  image[fn(x), fn(y)] := image[fn(x), fn(y)] + z(x, y, i);
  y := y + 4.0
end;
  x := x + 4.0;
end;
end;
  writeln;
end; { of MakeImage }

procedure StoreImage (image: imageType);
var
i, j: integer;
tb: char;
fname: string;
begin                           { store the calculated image on }
  writeln;                      { disk. SciHelper format is used }
  write('Output name ? ');      { by the freeware program Scientist's}
  readln(fname);                { Helper which was used to create }
  writeln;                      { many of the figures.            }
  write('(1) TEXT or (2) Scientist''s Helper format ? ');
  readln(i);
  if i = 1 then
tb := ' '
  else
tb := chr(9);
  rewrite(f, fname);
  if i = 2 then
writeln(f,'C1',tb,'C2',tb,'C3',tb,'C4',tb,'C5',tb,'C6',tb,'C7',
```

```
        tb,'C8',tb,'C9',tb,'C10',tb,'C11');
  for i := 1 to 11 do
begin
  for j := 1 to 11 do
write(f, image[i, j] : 5 : 1, tb);
  writeln(f);
end;
  close(f)
end; { of StoreImage }

procedure ShowImage (image: imageType);
var
    i, j: integer;
begin                              { show the image on the screen }
  for i := 1 to 11 do
begin
  for j := 1 to 11 do
write(image[i, j] : 5 : 1);
  writeln;
    end;
end; { of ShowImage }

begin  { MAIN PROGRAM }
ShowText;
zeroimage(image);
writeln('2D-Image, Makes a 2D image from the Gaussian model.');
writeln('--------  RTK, 06-16-93.');
writeln;
writeln;
write('Array center-to-center spacing (1 or 2 mm) ? ');
readln(i);
if i = 1 then
fill1mm(xi)
else
fill2mm(xi);
writeln;
write('Working ');
MakeImage(image);
StoreImage(image);
write(chr(12));
ShowImage(image);
writeln;
write('Press return to exit:');
readln
end.
```

C.2 Program 2. Simulate the Light Distribution of a Linear Fiber Array in 1 Dimension

Pascal program 2 was used to simulate the light distribution from a single linear fiber array with a center-to-center spacing of 1mm or 2mm when measured as a 1-dimensional cross section at a distance of 125mm from the face of the array. The output from this program was compared against measured data from single linear arrays of fibers. This program uses the generic Gaussian model for the light from a single fiber.

```
program GENERATE_SUM (input, output);

var
f: text;
    fname: string;
yn: char;
i, j, N: integer;
x, A, nn, max, Xlow, Xhigh, Xinc: double;
xx, yy, xi: array[1..100] of double;

begin
  repeat
write(chr(12));
    writeln('Generate a normalized sum of N Gaussians,
              n millimeters apart.');
writeln;
write('Enter the output file name: ');
readln(fname);
repeat
  writeln;
  write('Enter Xlow, Xhigh and Xinc: ');
  readln(xlow, xhigh, xinc);
until ((Xhigh - Xlow) / Xinc) <= 100; { keep number of points small }
writeln;
write('Enter the number fo fibers: ');
readln(N);
writeln;
write('Enter the fiber-to-fiber distance in millimeters: ');
readln(nn);
writeln;
write('Enter the generic fit parameter A = ');
readln(A);
writeln;
```

```
write('Working ');
if N mod 2 = 0 then    { fill in locations of fibers for even }
  for i := 1 to N do
 xi[i] := -((nn / 2) + (N / 2 - 1) * nn) + (i - 1) * nn
else
  for i := 1 to N do   { or odd number... }
 xi[i] := -((N - 1) / 2 * nn) + (i - 1) * nn;
x := Xlow;
i := 0;
max := -10000000;
while X <= Xhigh do
begin
  i := i + 1;
  yy[i] := 0;
  for j := 1 to N do
yy[i] := yy[i] + exp(-A * (x - xi[j]) * (x - xi[j]));
  if yy[i] > max then
max := yy[i];    { store maximum for normalizing }
  xx[i] := x;
  write('.');
  x := x + Xinc
end;
writeln;
writeln;
writeln('Normalizing data.');
for j := 1 to i do
  yy[j] := yy[j] / max;
writeln;
writeln('Storing data to ', fname, '.');
rewrite(f, fname);
for j := 1 to i do
  writeln(f, xx[j] : 10 : 4, chr(9), yy[j] : 10 : 4);
close(f);
writeln;
write('File complete, another ? ');
readln(yn)
  until (yn <> 'Y') and (yn <> 'y')
end.
```

C.3 Program 3. Sum the Measured Light Intensity in a Specified Region

Pascal program 3 displays the data measured from a 2-dimensional cross section and calculates the sum of intensities (in milliwatts) in a specified region.

```
program intensity_sum;
```

```
(*  Sums regions of 11 by 11 plots, RTK, 02-12-93. *)

type
arrayType = array[1..25, 1..25] of real;

var
a: arrayType;
f: text;
fname: string;
R: Rect;
left, top, right, bottom: integer;
x1, x2, y1, y2: integer;
Sum: real;

procedure load_file (var a: arrayType);  { read from a disk file }
var
i, j: integer;
begin
fname := OldFileName(' ');
writeln;
write('Loading file: ', fname, '...');
reset(f, fname);
readln(f);    { skip Scientist's Helper header line }
for i := 1 to 11 do
  begin
for j := 1 to 10 do
  read(f, a[j, i]);
readln(f, a[11, i]);
  end;
close(f);
end; { of load_file }

procedure init_windows;         { setup the Macintosh's windows }
begin
SetRect(R, 2, 40, 510, 355);
SetDrawingRect(R);
SetRect(R, 2, 360, 510, 382);
SetTextRect(R);
ShowText;
ShowDrawing;
end; { of init_windows }

procedure draw_table;
var
i, j: integer;
fnum: integer;
begin
ForeColor(redColor);            { draw the data in a window }
GetFNum('geneva', fnum);        { most of this is necessary to }
```

```
TextFont(fnum);                    { write to a window on the  }
TextSize(9);                       { Macintosh... }
MoveTo(2, 12);
WriteDraw(fname, ':');
ForeColor(greenColor);
TextFont(0);
TextSize(12);
for i := 1 to 11 do
  for j := 1 to 11 do
    begin
 MoveTo(20 + 40 * (j - 1), 48 + 20 * (i - 1));
 WriteDraw(a[j, i] : 4 : 0);
    end;
ForeColor(cyanColor);
for i := 1 to 11 do
  begin
    MoveTo(5, 48 + 20 * (i - 1));
WriteDraw(i : 2);
MoveTo(20 + 40 * (i - 1), 30);
WriteDraw(i : 4);
  end;
ForeColor(greenColor);
end;

procedure draw_box (top, left, bottom, right: integer);
begin
    ForeColor(magentaColor);
SetRect(R, (left - 1) * 40 + 20, (top - 1) * 20 + 34,
           (right - 1) * 40 + 53, (bottom - 1) * 20 + 52);
PaintRect(R);
end;

procedure erase_box;
begin
ForeColor(greenColor);
PaintRect(R);
end;

procedure Sum_region;
var                                       { Sum the intensities in }
i, j: integer;                     { a selected region }
begin
    Sum := 0;
for i := left to right do
  for j := top to bottom do
Sum := Sum + a[i, j];
end;

begin
PenMode(patXor);
```

```
PenSize(2, 2);
init_windows;
write('SOURCE file ?');
load_file(a);
draw_table;
repeat
  writeln;
  write('First point, 0 0 to exit (x,y): ');
  readln(x1, y1);
  if x1 = 0 then
halt;
  write('Second point (x,y): ');
  readln(x2, y2);
  if (x1 < x2) then
begin
  left := x1;
  top := y1;
  bottom := y2;
  right := x2;
end
  else
begin
  left := x2;
  top := y2;
  bottom := y1;
  right := x1;
end;
  draw_box(left, top, right, bottom);
  Sum_region;
  writeln;
  write('Sum in region is ', sum : 5 : 0, ', press return:');
  readln;
  Erase_box;
    until FALSE;
end.
```

C.4 Program 4. Find the Percent Difference Between 2 Dimensional Cross Sections

Pascal Program 4 was used to calculate the actual percent difference between measurements of the 2-dimensional cross section from single linear arrays of fibers. It allows for a matching of the peak of one file to the peak of the second to align the data.

```
program FindDiff (input, output);

{ Matches and compares 11 x 11 data sets   }

{ RTK, 11-22-92. For thesis.   }
{ Modified: 07-01-93, RTK      }

type
    bigdata = array[1..11, 1..11] of real;
    strng = string[80];

var
    F1, F2, A: bigdata;
    S1, S2, O, yy: strng;
    i, j, x, y, x1, x2, y1, y2: integer;
    xm, ym, yn: integer;
    ofile: text;

procedure readData (var A: bigdata; S: strng);
{ reads an 11 by 11 file }
var
    f: text;
    i, j: integer;
begin
    reset(f, S);
    readln(f);    { skip Scientist's Helper header }
    for i := 1 to 11 do
      begin
        for j := 1 to 10 do
          read(f, a[i, j]);
        readln(f, a[i, 11]);
      end;
    close(f);
end; { of readData }

procedure showData (A: bigdata);
var
    i, j: integer;
begin
    for i := 1 to 11 do
      begin
        for j := 1 to 10 do
          write(A[i, j] : 5 : 0);
        writeln(A[i, 11] : 5 : 0);
      end;
end; { of showData }

procedure SetWindow;
var
      r: rect;
```

```
begin
      SetRect(r, 2, 42, 510, 382);
      SetTextRect(r);
      ShowText;
end; { of SetWindow }

begin { Main }
   SetWindow;
   repeat
     for i := 1 to 11 do
       for j := 1 to 11 do
         A[i, j] := 0;
     write(chr(12));
     writeln('Find the percent difference between two
              11 by 11 data files.');
     writeln('========================================
              ====================');
     S1 := OldFileName(' ');
     S2 := OldFileName(' ');
     readData(F1, S1);
     readData(F2, S2);
     showData(F1);
     writeln;
     showData(F2);
     write('Enter point in first file [row,column]: ');
     readln(x1, y1);
     write('Enter point to match to in second file: ');
     readln(x2, y2);
     write(chr(12));
     writeln('Matching files and computing percent differences...');
     for x := 1 to 11 do
       for y := 1 to 11 do
         begin
           xm := x + x2 - x1;
           ym := y + y2 - y1;
           if (xm < 1) or (xm > 11) then
             begin
               A[x, y] := 1000;
               cycle
             end;
           if (ym < 1) or (ym > 11) then
             begin
               A[x, y] := 1000;
               cycle
             end;
           A[x, y] := 100 * (F1[x, y] - F2[xm, ym]) / F2[xm, ym];
         end;
     writeln;
     write('Output table to (0) screen or (1) file ? ');
     readln(yn);
```

```
      writeln;
      writeln;
      if yn = 1 then
        begin
          O := NewFileName('Write table to...', 'Diff. Table.DIF');
          rewrite(ofile, O);
          for i := 1 to 10 do
            write(ofile, 'Col', i : 2, chr(9));
          writeln(ofile, 'Col11');
          for x := 1 to 11 do
            begin
              for y := 1 to 10 do
                write(ofile, A[x, y] : 6 : 1, chr(9));
              writeln(ofile, A[x, 11] : 6 : 1);
            end;
          close(ofile);
        end
       else
        begin
          for x := 1 to 11 do
            begin
              for y := 1 to 10 do
                begin
                  if A[x, y] = 1000.0 then
                    write('   ***')
                  else
                    write(A[x, y] : 6 : 1);
                end;
                if A[x, y] = 1000.0 then
                  writeln('   ***')
                else
                  writeln(A[x, 11] : 6 : 1);
            end;
         end;
       writeln;
       write('Another file ? ');
       readln(yy);
   until (yy = 'N') or (yy = 'n');
end.
```

Bibliography

[Cherin1] A. H. Cherin, *An Introduction to Optical Fibers*, McGraw-Hill, New York, 1983, p. 2.

[Newport2] *The Newport Catalog with Applications No. 100*, Section on Fiber Basics, p. J-2.

[Newport3] *The Newport Catalog with Applications No. 100*, Section on Fiber Basics, p. J-2.

[Cherin4] A. H. Cherin, *An Introduction to Optical Fibers* McGraw-Hill, New York, 1983, p. 8.

[Newport5] *The Newport Catalog with Applications No. 100*, Section on Fiber Basics, p. J-2.

[Newport6] *The Newport Catalog with Applications No. 100*, Section on Fiber Basics, p. J-3.

[Newport7] *The Newport Catalog with Applications No. 100*, Section on Fiber Basics, p. J-3.

[Newport8] *The Newport Catalog with Applications No. 100*, Section on Fiber Basics, p. J-3.

[Ford9] Handout given by Ford personnel at a meeting between Ford and Michigan State, November 1, 1990.

[Ford10] Private communication from Ford personnel.

[Ford11] Private communication from Ford personnel.

[Ford12] Illustration used by Ford personnel at a meeting between Ford and Michigan State, May 1991.

[Time13] *The Time-Life Book of the Family Car*, Time-Life, p. 183.

[Sentinel14] *"Marque X - Contemporary, Luxury Convertible"*, The Milwaukee Sentinel, Saturday, July 10, 1993.